I STRESS-STRAIN-STRENGTH BEHAVIOR OF COHESIONLESS SOILS

(Plus 3 pages of mini-problems on (un)drained shear & structure)

Sheets: MFS-4 to 10

Mini-Problem / Questions on Drained Shear of Sands (Review)

1) What is the difference (if any) between

a) • constant volume ϕ'_{cv}
• steady state ϕ'_{ss}
• critical state ϕ'_{cs} ?

b) Can CD & CU tests be used with equal confidence to obtain CSL/SSL
. for $+\psi$?
. for $-\psi$?

2) In Rowe's (1962) model of strength components:

a) What is the physical significance of ϕ'_f and how is it obtained?

b) How do ϕ'_p & ϕ'_f vary as a $f(\psi)$ for CIDC(L) tests?

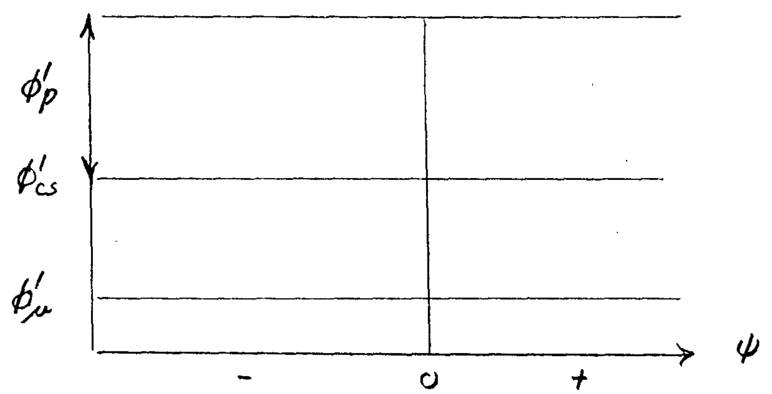

3) How does $d\phi'_p / d\log\sigma'_{ct}$ (pressure sensitivity) vary with increasing

a) D_r b) D_{50} c) Particle crushing strength?

4) What are the main problems in estimating ϕ'_p (TC) for a natural SW-SM sand

a) Using correlations with ψ?
b) Using Bolton's (1986) eqn?

5) For the MIT-S1 model of sand behavior:

a) What does it use to replace the VCL of clays and how is this reference line obtained?

b) How good is it at predicting for Toyoura sand:
(1) The location of the CSL?
(2) ϕ'_p & RD vs $\log\sigma'$ as $f(D_r)$ compared to Bolton (1986)?

5/3/99 5/01
5/99

Mini-Problem/Questions on Undrained Shear of Sands

1) Four different shaped stress-strain curves are plotted below, along with four different ESPs, from CIUC tests.

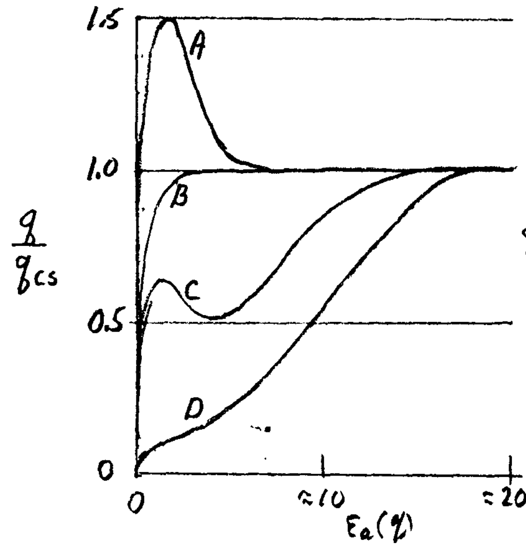

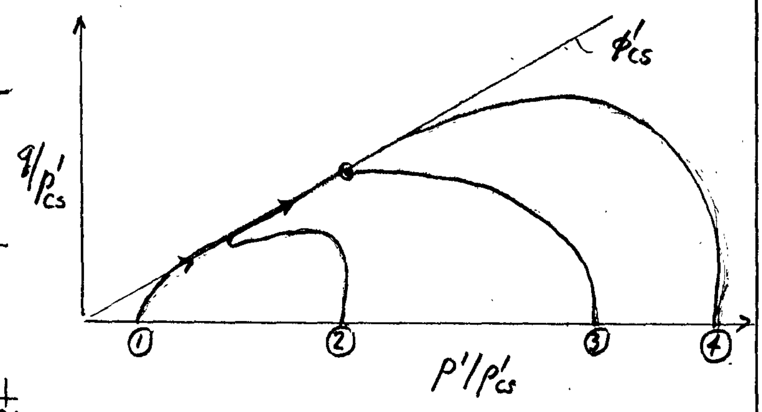

a) Identify q_Y, q_{QSS} & q_p on each curve.

b) Match the $q-\varepsilon_a$ and ESPs (which no. goes with which letter?)

c) What conditions of D_r & σ_c' lead to each curve based on the MIT-S1 predicted behavior for Toyoura sand?

d) Make qualitative estimates of ψ for each curve.

2) According to MIT-S1 model, for large $+\psi$:

CAU $K_c = 0.5$

a) CIUC → CAUC → what changes in q_p/σ_{vc}', ε_p, ϕ_p' and ϕ_{cs}'?

b) CIUE → CAUE → " " " " " " " "

"

c) How do q_p/σ_{vc}' from CIUC vs CIUE & from CAUC vs CAUE compare to data on NC clays?

Mini-Problem on Effects of Sand Structure

1) Do K_0-Consolidated sands have a structure with aspects similar to those of clays?

2) Regarding the inherent anisotropy of sands:

a) What testing data are shown to illustrate it's effects?

b) How do the trends compare with those for clays?

3) a) What is induced anisotropy?

b) Which shear device has been used to illustrate its importance?

c) Does the "softest" response occur at the same angle as for inherent anisotropy?

4) If one prepares sand samples in the lab that have the same density and "preconsolidation pressure" as an in situ sand, should it have the same basic stress-strain behavior?

5) Be prepared to discuss sands vs clays regarding:

a) Basic behavioral trends
- Effects of σ̄ & δ
- Parameters to unify stress-strain behavior

b) Practical differences
- Role of drainage & capillary stresses
- Estimation of properties
- Predictions & importance of:
  - settlement
  - stability
  - lateral earth pressures

NOTES FROM 1.361-1.366 FOR SECTION 1 = DRAINED SHEAR

III-2 STRESS-STRAIN-STRENGTH PROPERTIES

Page No

Sheets

A: CIDC(L) data on loose & dense sand as f(σ')
B: Particle crushing
C1, 2: State Parameter ψ
D: Bolton (1986)
E1-4: MIT-S1 model & shear data
F: Effect of b & sample preparation

3.4 Effect of Relative Density (Illustrated via Std. TC tests)

(1) Stress-strain data ($\sigma = \phi'$)

——— Dense, - - - - Loose } $\sigma'_c = \sigma'_{3f} = 1$ atm

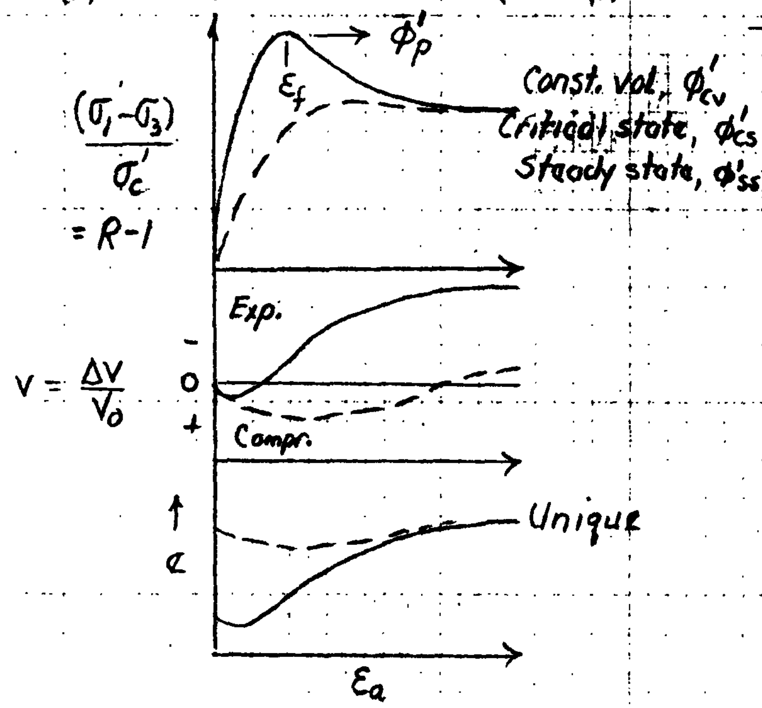

Dense

- Small ε_f
- Significant strain softening
- Initial small contraction, then large expansion (dilation)

Loose

- Large ε_f
- Little strain softening

For Both at Critical = Steady State

* Unique $e - q - p$ condition
* with continued shearing
[Called Critical State Line = Steady State Line]

(2) Variation in ϕ'

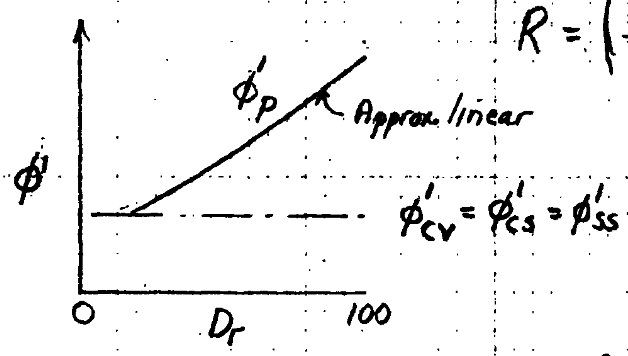

$$R = \left(\frac{\sigma_1}{\sigma_3}\right) = \tan^2(45 + \phi/2) = \frac{(1 + \sin\phi')}{(1 - \sin\phi')}$$ } L&W Fig. 11.5

Also $\sin\phi' = (R-1)/(R+1)$

3.5 Three Components of Strength (Rowe, 1962; differs from L&W)

(1) Frictional resistance

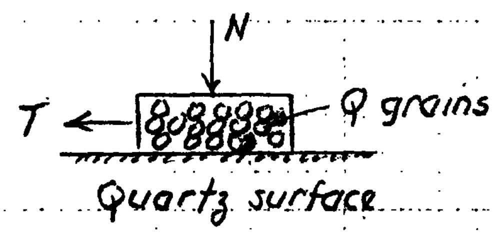

- Coef. of friction $\mu = T/N = \tan\phi'_\mu$
- Rowe (1962) states that ϕ_μ due to sliding only
- But more recent research indicates that also rolling at high ϕ'_μ (Skinner, 1969, Geot.)

(2) Resistance due to Dilation

- Component due to expansion of soil during shear against the confining stresses (expansion from "interlocking")
- Magnitude is proportional to rate of volume change $\varepsilon_{vol} = \frac{\Delta V}{V_0} = \dot{V}$

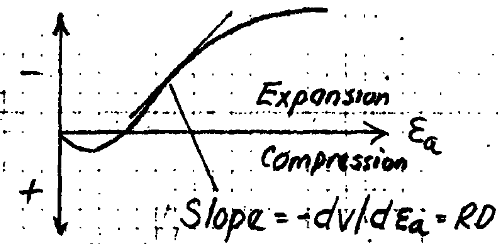

- $R_p = \left(\frac{\sigma_1'}{\sigma_3'}\right)_{max} = (1 + RD)\underbrace{\tan^2\left(45 + \frac{\phi_f'}{2}\right)}_{R_f}$

($\left(\frac{\sigma_1'}{\sigma_3'}\right)_{max}$: MEASURED; RD: BACKCALCULATED)

NOTE: ϕ_p' occurs at max. slope

(3) Resistance due to Interference

- "Interlocking" also results in fact that sand particles cannot move in a straight line, but must go around each other
- At const. vol. ($dv/d\varepsilon_a = 0$) → $\tan\phi_{cs}' \approx \frac{\pi}{2}\tan\phi_\mu'$

($\frac{\pi}{2} = \frac{1}{2}$ circumference / diameter) (really not that simple)

(4) Summary

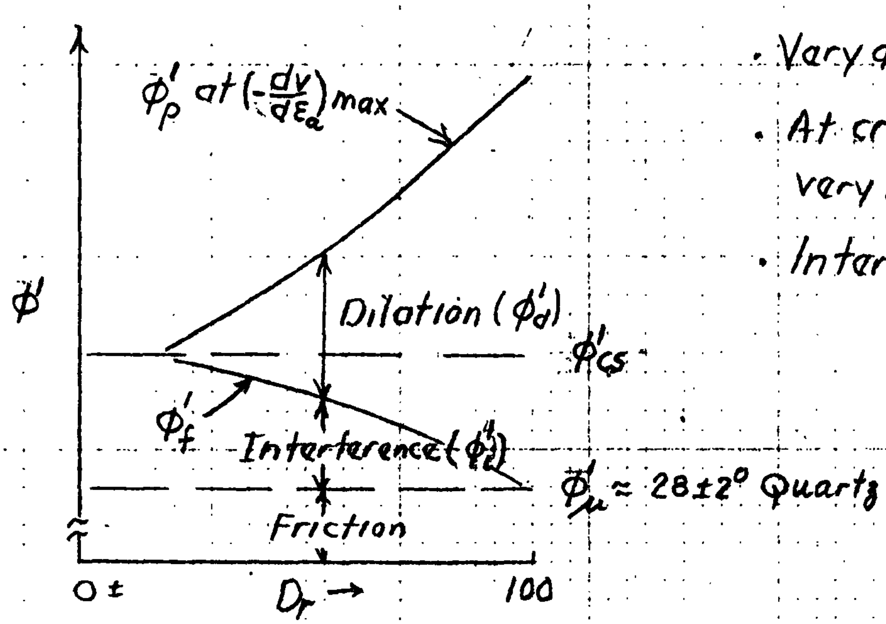

- Very dense: $\phi_p' = \phi_\mu' + \phi_d'$
- At critical state and very loose: $\phi_p' = \phi_{cs}' = \phi_\mu' + \phi_i'$
- Intermediate: $\phi_p' = \phi_\mu' + \underbrace{\phi_i' + \phi_d'}_{L \,\&\, W \text{ "interlocking"}}$

NOTE: ϕ_f' calculated from measured ϕ_p' (i.e. R_{max}) & max. $(-dv/d\varepsilon_a)$

4. COMBINED EFFECTS OF DENSITY AND CONFINING PRESSURE ON STRENGTH OF GRANULAR SOILS

4.1 Overview of Data From Standard Triaxial Compression Tests

1) Effect of confining stress level on stress-strain behavior of dense sand (idealization of data shown in Fig. 3 of Sheet A)

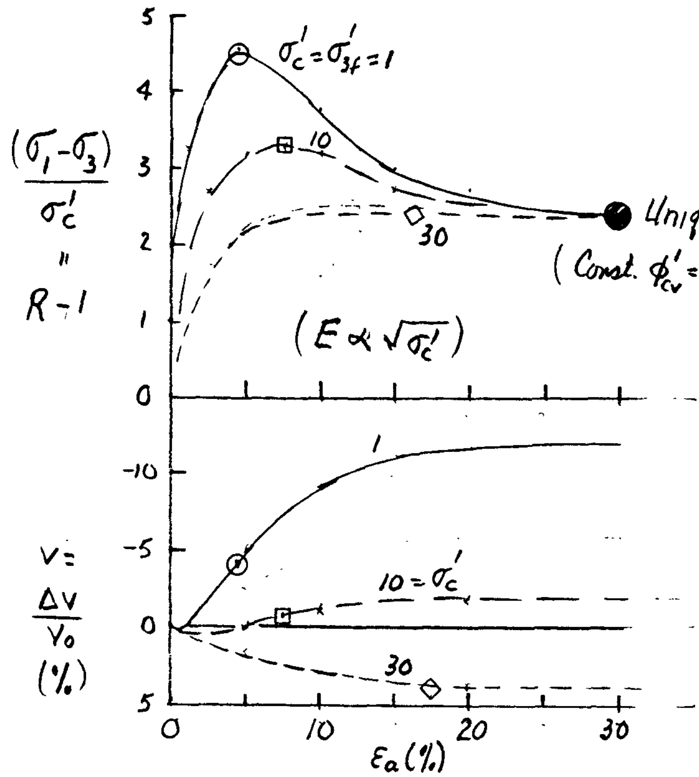

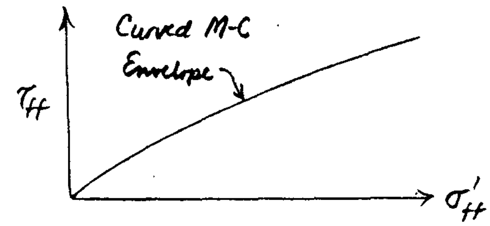

Trends for Increasing σ_c'

- Increasing ε_f (ε at peak)
- Less expansion (dilation) to only compression (contraction)
- Lower max rate of dilation ($RD = -dv/d\varepsilon_a$)
- Decreasing ϕ_p'

∴ Same basic trends as effect of decreasing D_r at low σ_c'

2) Peak friction angle (ϕ_p') vs. confining stress at failure (see Fig III 2-1, p 9a)

- See large variation in "pressure sensitivity" ($d\phi_p'/d\log\sigma_{oct}'$) for different densities and type of granular soil
- In general, larger pressure sensitivity
  - With increasing D_r, e.g. data of Lee & Seed (1967) and Vesic & Clough (1968)
  - With weak sand grains, e.g. Ottawa (Quartz) sand → calcareous sand

∴ Therefore related to compressibility of test material

Note: $d\phi_p'/d\log\sigma' \rightarrow$ 5-10° for rockfill, very dense sand & gravel and for calcareous soils (even when loose, see Line D in Fig. III 2-1)

CCL 9/19/95 25 9/96

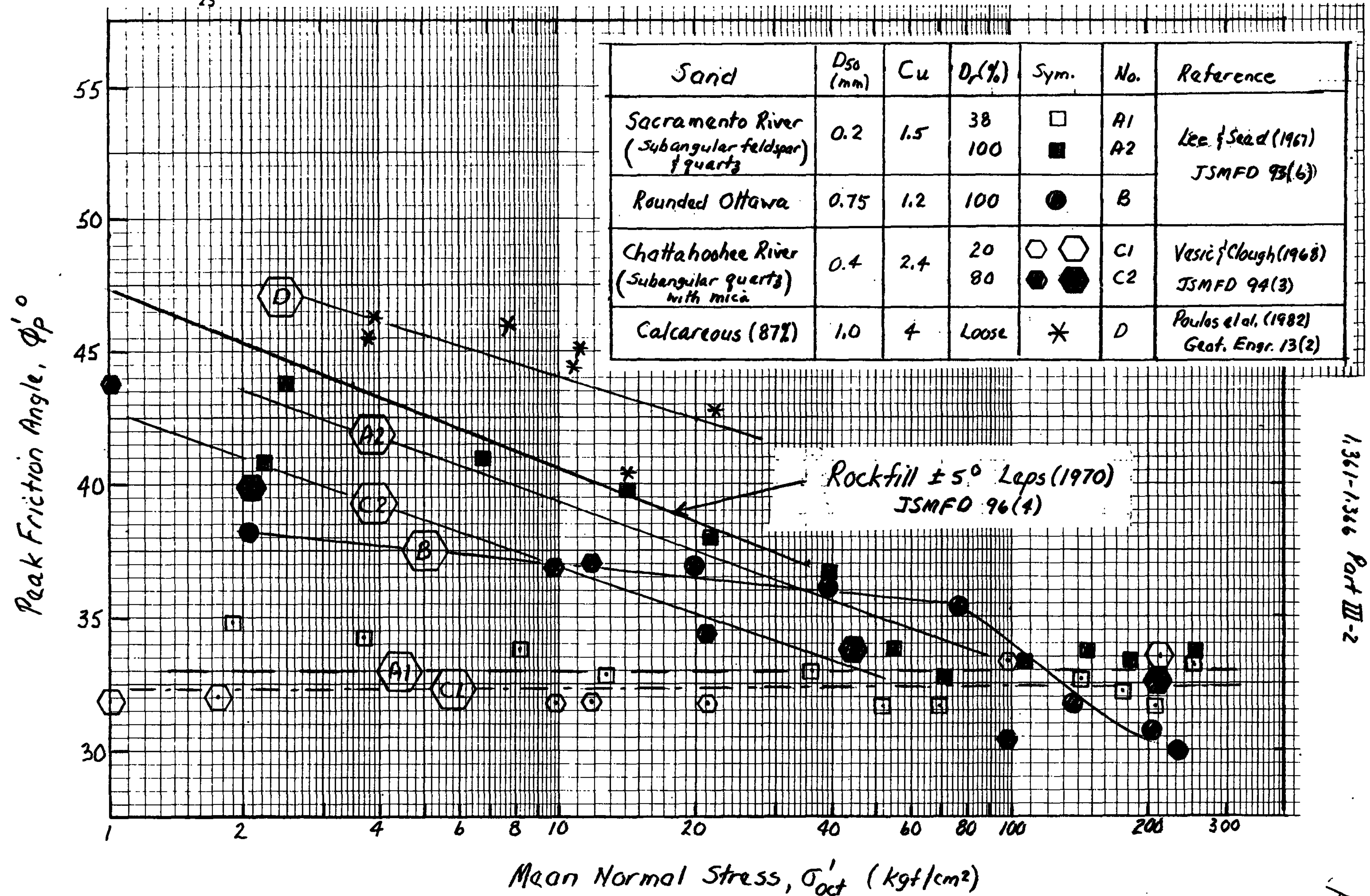

Sand	D_{50} (mm)	Cu	D_r(%)	Sym.	No.	Reference
Sacramento River (Subangular feldspar & quartz)	0.2	1.5	38	□	A1	Lee & Seed (1967) JSMFD 93(6)
			100	■	A2	
Rounded Ottawa	0.75	1.2	100	●	B	
Chattahoohee River (Subangular quartz with mica)	0.4	2.4	20	⬡ ⬡	C1	Vesic & Clough (1968) JSMFD 94(3)
			80	⬢ ⬢	C2	
Calcareous (87%)	1.0	4	Loose	*	D	Poulos et al. (1982) Geot. Engr. 13(2)

Fig. III 2-1 Effect of Stress Level on Peak Friction Angle of Loose and Dense Granular Materials

3) Particle crushing

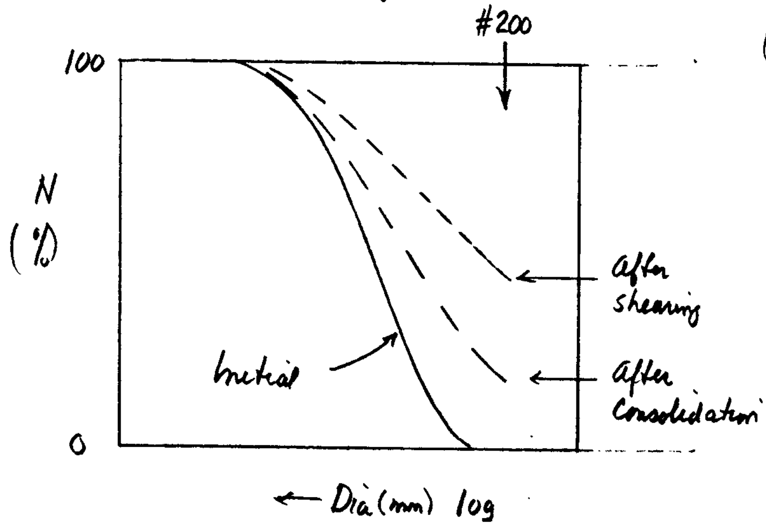

(See Sheet B for actual data)

Dense Ottawa: little crushing at σ'_c = 40ksc and low pressure sensitivity

Dense Chattahoochee & Sacramento River Sands: alot of crushing and high pressure sensitivity

4) Strength components of dense sand with increasing confinement

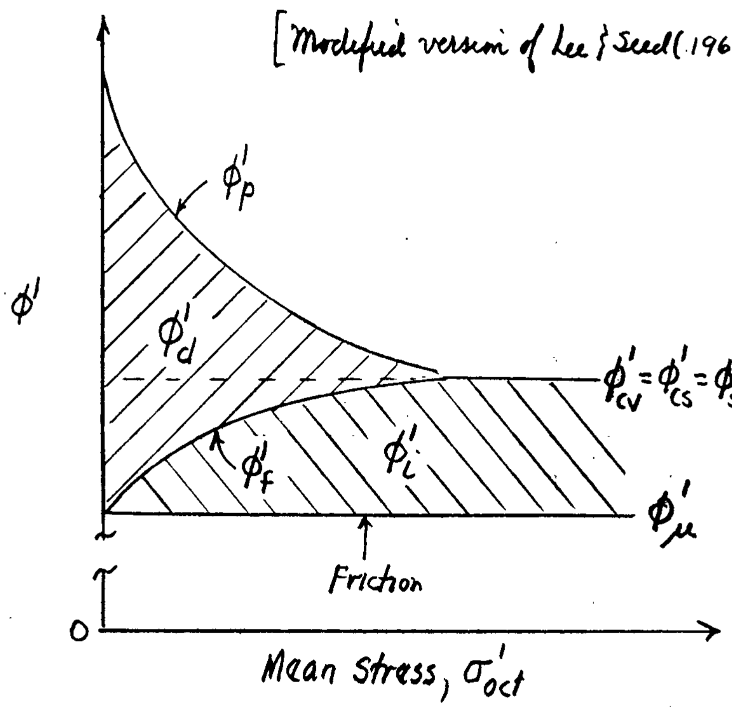

$R_p = \tan^2(45 + \phi'_p/2)$

$R_f = \tan^2(45 + \phi'_f/2)$

Rowe (1962)

$R_p = (1 + RD)\, R_f$

Bishop (1954) & Taylor (1948)

$R_p = RD + R_f$, i.e. predicts smaller effect of dilation where $RD = \max(-dv/d\varepsilon_a)$

Notes: (1) ϕ'_i = interference + particle crushing

(2) At very high σ'_{oct}, may require very large strains to reach CSL = SSL (e.g., see Fig. 5.27, Sheet E3)

Will next look at three different approaches for evaluating the combined effects of density and confinement on stress-strain-strength of sands

4.2 State Parameter, ψ (Been & Jefferies 1985; Been et al. 1991)

1) Definition

$\psi = e - e_{ss}$ at same σ'_{oct}, i.e., SSL = reference state

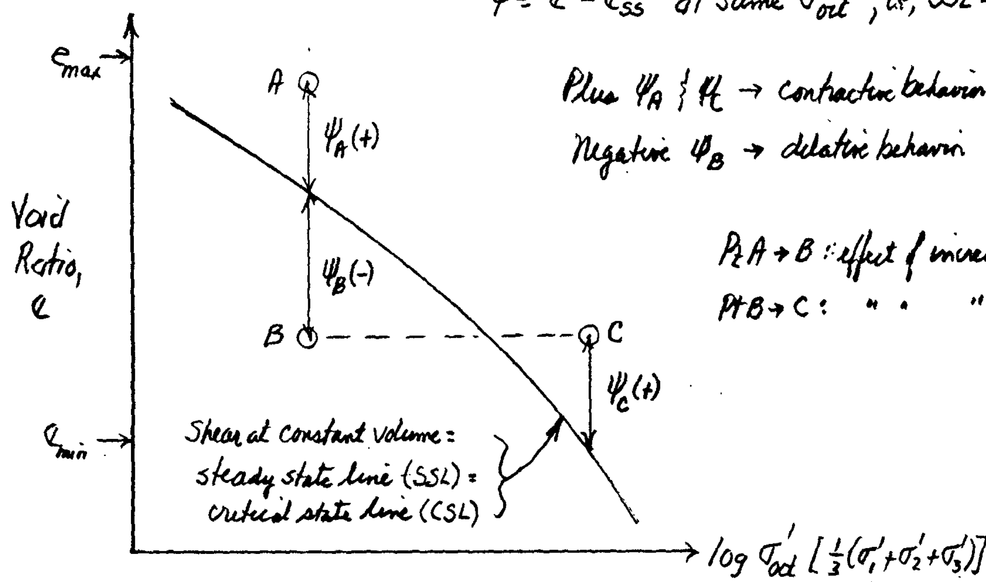

Plus ψ_A & ψ_C → contractive behavior } during shear
Negative ψ_B → dilative behavior }

Pt A → B: effect of increasing D_r
Pt B → C: " " " σ'

2) Examples of "unique" correlations between ψ and shear behavior

See Sheet C1 for actual correlations:

- Fig 14: Decreasing ψ → increasing rate of dilation at peak strength
- Fig 15: " " " " $\phi'_p - \phi'_{ss}$ ($\phi'_{ss} = \phi'_{cv} = \phi'_{cs}$) } ± 2-3°
- Fig 16: " " " " ϕ'_p

3) Problems with application in practice

a) Slight variations in particle size distribution can have a large effect on location of the SSL, e.g. Sheet C1, Fig. 7 for uniform medium sand with 0, 2, 5 & 10% fines (-#200)

b) Whether or not drained vs undrained shear from ± ψ will produce the same SSL = CSL is still controversial. Sheet C2, Fig. 12 indicates that drained shear with $-\psi$ does not reach SSL (maybe due to non-uniform conditions (shear planes) in test specimens)

c) Get marked curvature in CSL at stresses → significant crushing, e.g. Sheet C2, Figs. 8, 11 & 12

CCL Conclusion: Excellent concept (especially for teaching), but difficult to use quantitatively in practice

4.3 Semi-Empirical Correlations (Bolton 1986)

1) Approach: Evaluated drained TC and PS (plane strain) shear data from 17 test programs (Sheet D, Table 1) to determine effects of D_r and σ' level on max. rate of dilation and especially $\Delta\phi' = \phi'_p - \phi'_{cs}$ ($\phi'_{cs} = \phi'_{cv}$).

2) Results of study (for tests that dilate during shear, i.e., start with $\psi < 0$) led to I_R = relative dilatancy index (Note: at σ' ↑ → significant crushing)

$$I_R = D_r(10 - \ln\sigma'_f) - 1 \quad \text{where } D_r = \text{relative density (decimal)}$$
$$\sigma'_f = \sigma'_{oct} \text{ at failure in kPa}$$

3) Resulting correlations for Std. TC [CIDC(L)]

$$\left.\begin{array}{l}\Delta\phi' = \phi'_p - \phi'_{cs} = 3 \cdot I_R^{\circ} \text{ and Max. } RD = 0.3 I_R \\ \text{(Note: For plane strain, } \Delta\phi' = 5 \cdot I_R^{\circ}\text{)}\end{array}\right\} 0 < I_R < 4$$

4) Examples of predictions vs. measured data (See Sheet D)
- Fig. 7 Effect of increasing D_r on $\Delta\phi'$ and max. RD at $\sigma'_{oct} \approx 300$ kPa (both TC & PS)
- Fig 9 Effect of increasing D_r on $\Delta\phi'$(TC) at $\sigma'_{oct} = 20, 50, 100$ & 600 kPa (quite good)
- Fig. 10 Effect of increasing σ'_{oct} at varying D_r on $\Delta\phi'$ (TC)

5) Bolton (1986) also suggests that: typical error in $D_r = \pm 5\%$; for mainly quartz grains, $\phi'_{cs} = 33° \pm 1\text{-}2°$; for feldspar grains, $\phi'_{cs} \approx 40°$

6) Pestana (1994) concludes from results in Section 4.4 that $\Delta\phi'$(TC) is reasonable at $\sigma'_{oct} > 100$ kPa, except when $D_r \to 100\%$. But $\Delta\phi'$(PS) is too high

4.4 Soil Model MIT-S1 (J. Pestana 1994 ScD Thesis)

1) Background on formulation for granular soils

- Uses Limiting Compression Curve (LCC) = linear portion of log e vs log σ'_{vt} compression curve at high stresses where particle crushing predominates as the reference state (like VCL for clays).
  See Sheet E1, Fig. 2.2 & 2.5
- For shear behavior, starts with "basic" elasto-plasticity theory (à la MCC), but adds alot of new features to incorporate hysteresis, anisotropy, strain softening, etc. See Sheet E1, Fig. 4.8

2) Input parameters for Toyoura Sand and some remarks

a) See Sheet E2, Table 5.2 for testing to obtain 14 parameters. Main tests are:

- Compression test to high σ'_c to define location of LCC with U/R cycle (hysteresis) and values of K_0
- Undrained TC test from σ'_c on LCC } shape of bounding surface, ϕ'_p &
- Drained TC test at low σ'_c } ϕ'_{cs}, etc.
- Resonant column to get small strain stiffness

b) Sketch of Sheet E2, Fig. 5.4 & 5.24

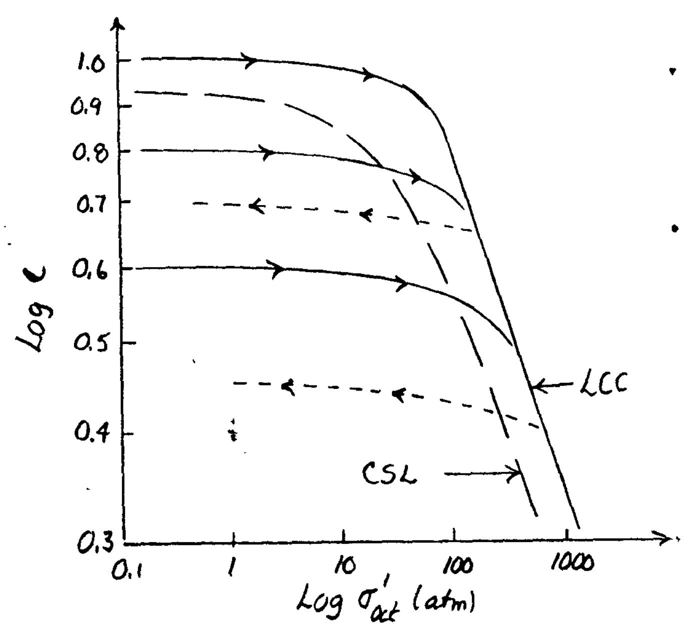

- Using input data from a test at one e_0 predicts compression & unloading at all values of e_0
- Also predicts location of the critical state line (CSL) !

3) Prediction of drained TC shear behavior of Toyoura Sand

a) Effect of varying D_r at low $\sigma_c' = 100$ kPa ($\approx$1 atm)
Sheet E3, Fig. 5.26

b) Effect of varying σ_c' at $e_0 = 0.8$ ($D_r = 45\%$)
Sheet E3, Fig. 5.27

c) Combined effects of varying D_r and σ_c' on ϕ_p'
Sheet E4, Fig. 5.28 Note $\approx$ linear ϕ_p' vs e_0 at constant σ_c'

d) Comparisons with Bolton's (1986) empirical eqn for ϕ_p' and RD
Sheet E4, Fig. 5.29 → rather remarkable agreement

NOTE: Most of the measured triaxial compression shear data on Toyoura Sand are from undrained shear tests. Comparison of predicted vs. measured behavior is covered in 1.322 (Soil Behavior)

5. OTHER FACTORS AFFECTING THE STRENGTH OF GRANULAR SOILS

5.1 Intermediate Principal Stress (σ_2)

1) Field conditions leading to different values of $b = \frac{(\sigma_2 - \sigma_3)}{(\sigma_1 - \sigma_3)}$

℄ Circular Footing	℄ Circular Excavation	℄ Strip Footing

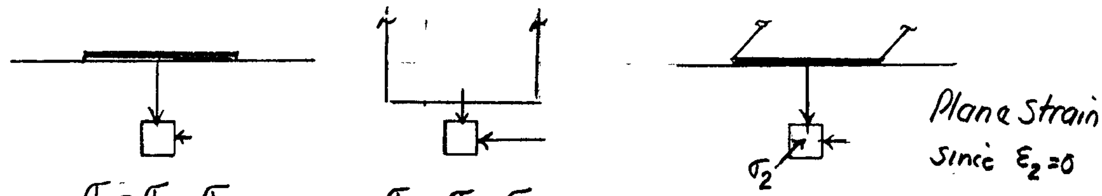

$\sigma_2 = \sigma_3 = \sigma_h$	$\sigma_2 = \sigma_1 = \sigma_h$	$\sigma_1 > \sigma_2 > \sigma_3$
TC, b = ___	TE, b = ___	PS, b ≈ 0.25-0.4

2) Device to measure the effect of varying b = True Triaxial
(very complex apparatus due to "corner" conditions)

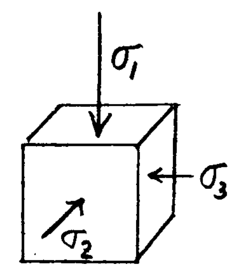

3) Some experimental results (Sheet F, Fig. 13)

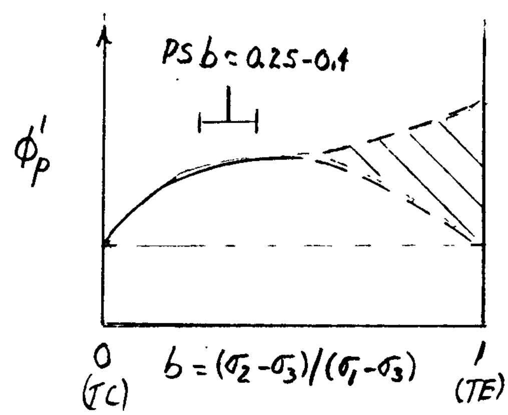

a) Conflicting data as $b \to 1$, probably due to experimental problems.
Note: MIT-S1 uses $\phi'_{TC} = \phi'_{TE}$

b) All data show increase in ϕ'_p as b increases from zero (TC) to b for $\varepsilon_2 = 0$ (PS = plane strain)

c) Comparison of ϕ'_{PS} vs. ϕ'_{TC} (of greatest practical importance)

- Bolton (1986) recommends $\Delta\phi' = \phi'_p - \phi'_{cs} = 3 \cdot I_R{}^{\circ}$ for TC
  $= 5 \cdot I_R{}^{\circ}$ for PS
  Hence $\phi'_{PS} - \phi'_{TC}$ increases with increasing D_r & decreasing σ'_{oct} (decr. ψ) à la Sheet D, Fig. 7
- CCL recommends Bolton (1986). Therefore
  $\phi'_{PS} - \phi'_{TC} \approx 0$ for low D_r - high σ'_{oct} ($\psi \geq 0$)
  $\approx 5^{\circ}$ for high D_r - low σ'_{oct} ($\psi << 0$)

4) Comments • Bolton assumes same ϕ'_{cs} for TC & PS, whereas Pestana (1994) concludes (correctly) that PS → higher ϕ'_{cs}
 • Part III-4 will show that $\Delta\phi' = +5°$ → doubling of q_{ult} (bearing capacity)

5.2 Method of Sample Preparation

1) Most lab shear tests on sand are run on reconstituted samples. The two most common methods are:
 • Pluviation, with or without vibration → more like natural deposits
 • Tamping (compaction) of moist soil → non-uniform density

2) Sheet F, Fig. 4 show example of very different stress-strain behavior (even though $\phi'_p \approx$ constant)

5.3 Anisotropy

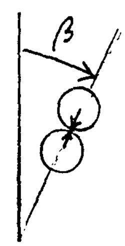

1) 1-D deposition leads to a sand structure with
 • Preferred orientation of elongated grains ⊥ to σ'_v (fabric)
 • " " " particle contacts (even with perfect spheres). See Sheet G, Fig. 8.15

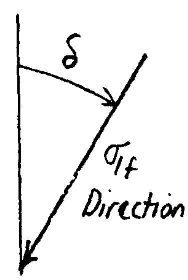

2) Hence natural sand (deposit) has an inherent anisotropy wherein shearing at different δ angles leads to different stress-strain-strength properties
 • Shearing at $\delta = 0°$ → highest modulus & ϕ'_p
 • Increasing δ → lower modulus & ϕ'_p

3) Examples of trends (Sheet G)
 • Fig. 2 ϕ'_p vs. δ for several sands ($\Delta\phi' \approx 3 \pm 1°$)
 • Fig 8 Effect of δ on ε_a vs $(\sigma_1 - \sigma_3)$ & ε_{vol} for dense sand

Data from Lee & Seed (1967, JSMFD, 93 (SM6)) : CIDC (L) = Std. Triax. Compr.

PRESSURE-VOID RATIO CURVES FOR SAND AT FOUR INITIAL DENSITIES

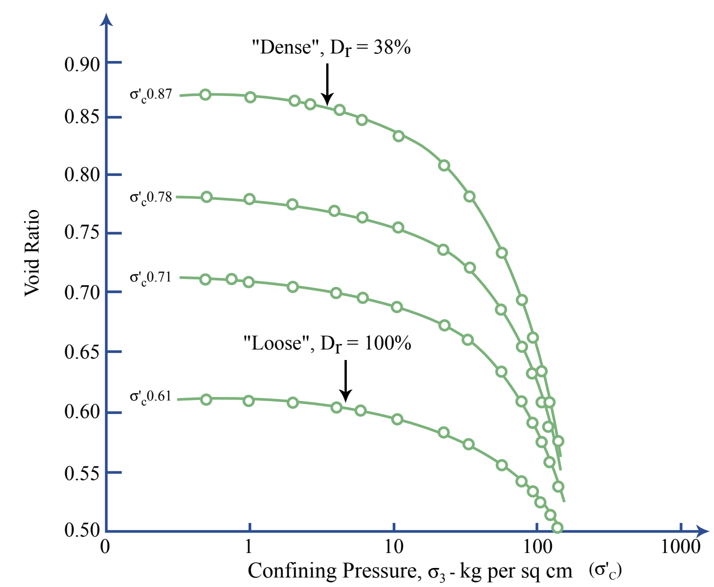

Sacramento River Sand
Three dimensional compression under uniforms confining pressures.
Equilibrium condition determined after 2 hours.

Sacramento River Sand

Subangular feldspar & quartz (#50-100)

$D_{50} = 0.2$ mm, $C_u = 1.5$

$e_{max} = 1.03$

$e_{min} = 0.61$

Note: D_r refers to initial density prior to consolidation

Figure by MIT OCW.

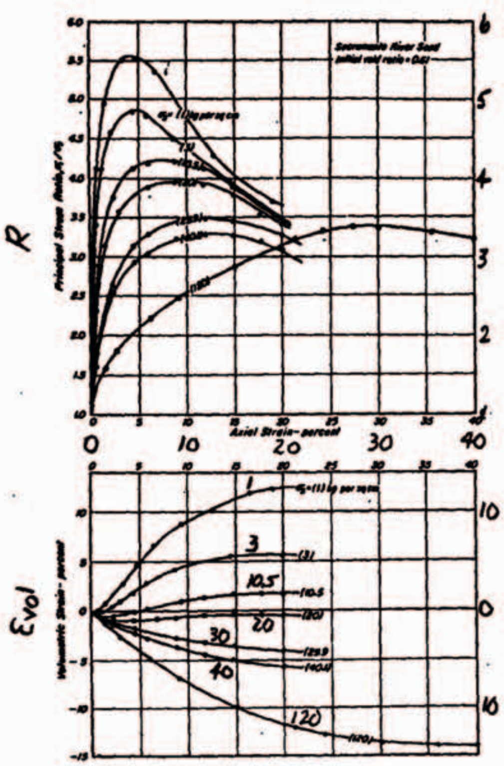

FIG. 3.—STRESS-STRAIN-VOLUME CHANGE DATA FOR DENSE SAND $D_r = 100\%$

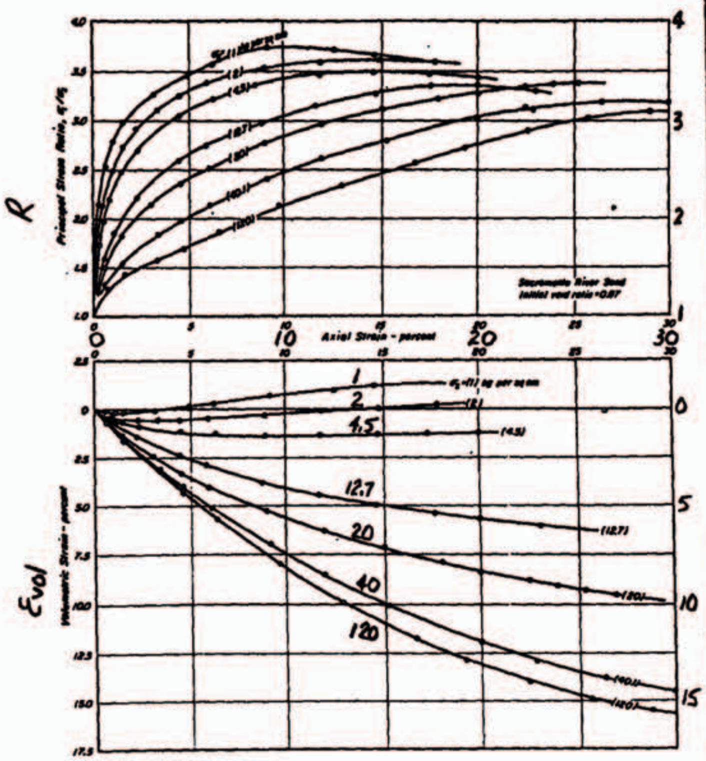

FIG. 4.—STRESS-STRAIN-VOLUME CHANGE DATA FOR LOOSE SAND $D_r = 38\%$

A

Data from Lee & Seed (1967, JSMFD, 93 (SM6)) : CIDC (L) = Std. Triax. Compr.

PRESSURE-VOID RATIO CURVES FOR SAND AT FOUR INITIAL DENSITIES

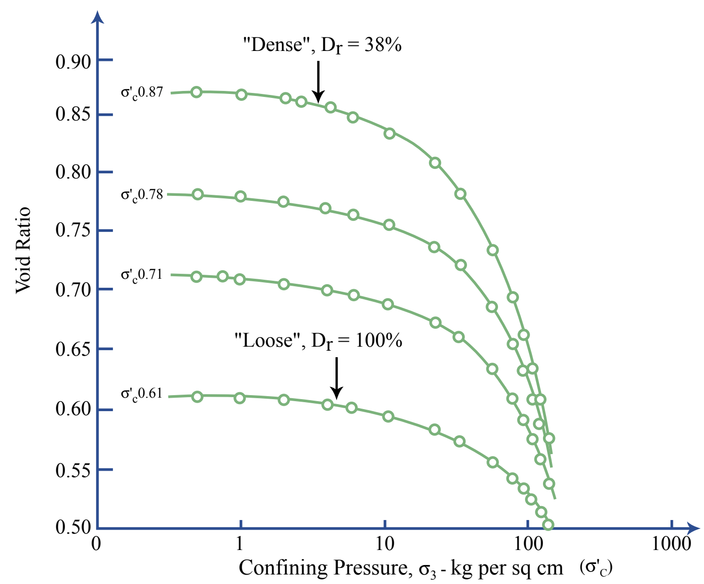

Sacramento River Sand
Three dimensional compression under uniforms confining pressures.
Equilibrium condition determined after 2 hours.

Sacramento River Sand

Subangular feldspar & quartz (#50-100)

D_{50} = 0.2 mm, C_u = 1.5

e_{max} = 1.03

e_{min} = 0.61

Note: D_r refers to initial density prior to consolidation

Figures by MIT OCW.

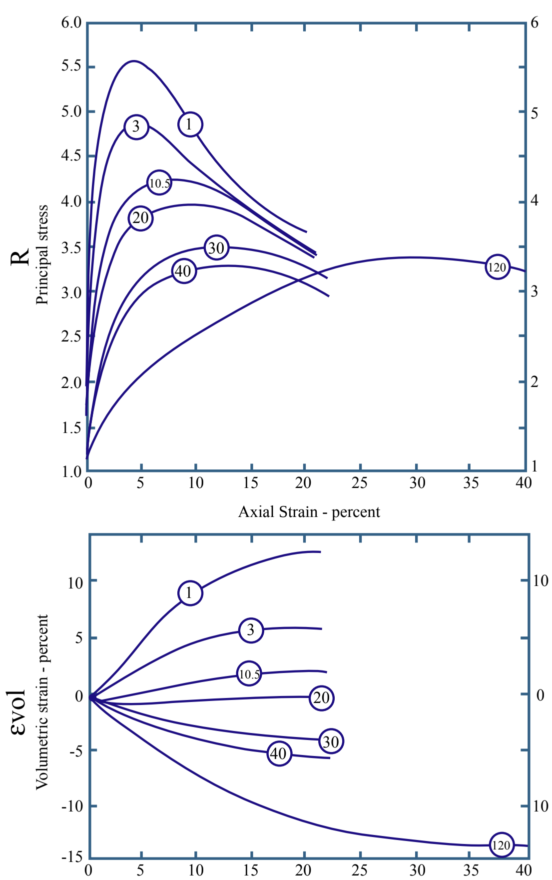

Stress-Strain-Volume change data for dense sand.

D_r = 100%

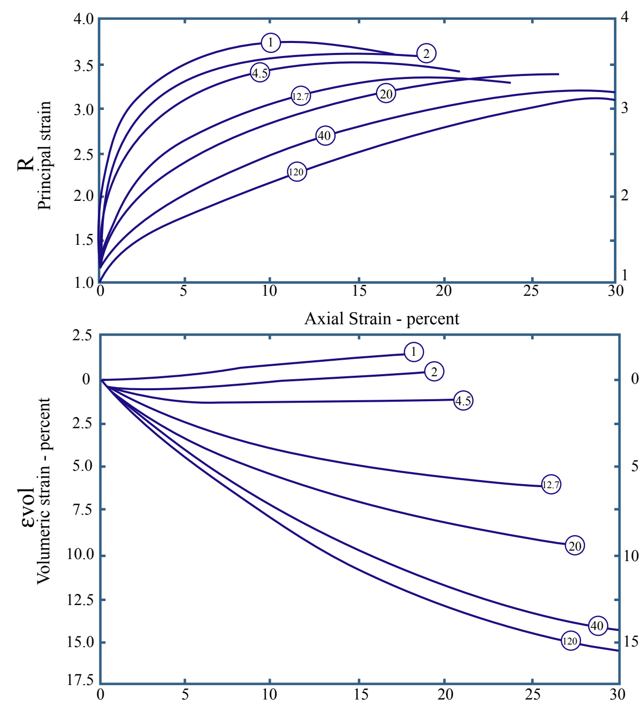

Stress-Strain-Volume change data for loose sand

D_r = 38%

Information of Particle Crushing

Adapted from Vesic & Clough (1968) for Chattahoochee River Sand

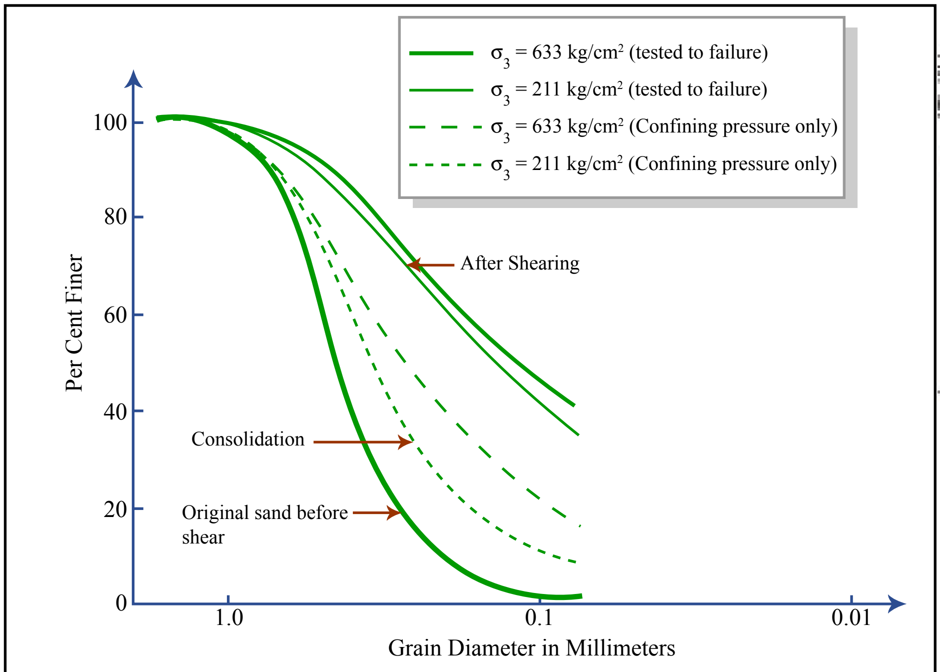

The Relative Continuation of Isotropic Compression and Shear on Breakdown

Figure by MIT OCW.

Adapted from Lee & Seed (1967) for Ottawa and Sacramento River Sand

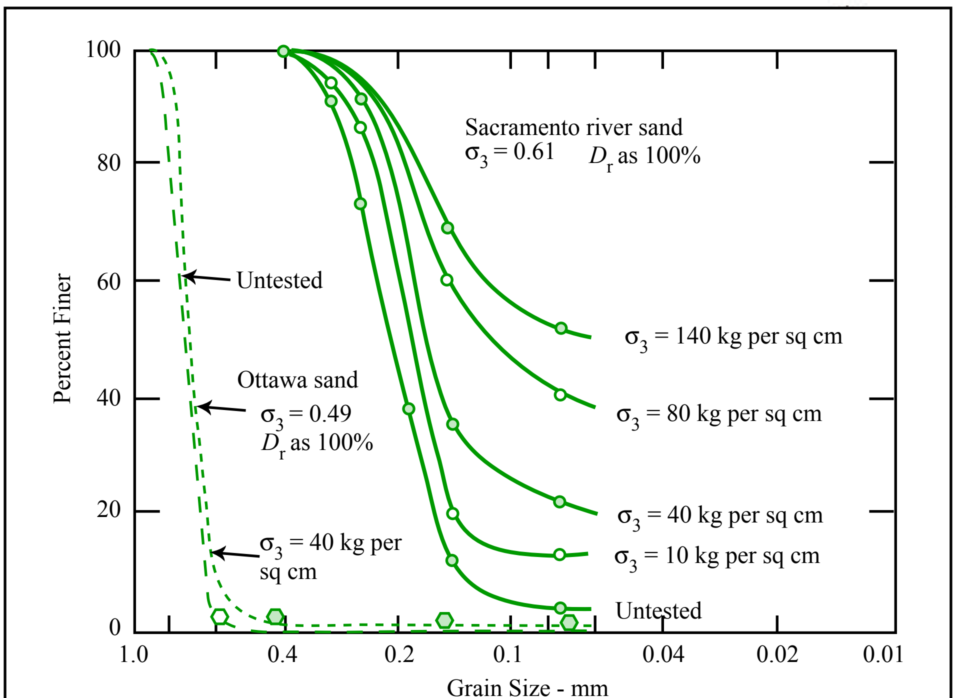

Degradation of dense sands After Drained Triaxial Tests

Figure by MIT OCW.

Data from Been & Jefferies (1985) Geotechnique 35(2), 99-102

Table 1. Index properties of Kogyuk sands

Sand–silt mixtures*	350/0	350/2	350/5	350/10
Median grain size D_{50}: mm	0·350	0·350	0·360	0·340
Percentage passing 200 sieve	0	2·2	5·5	9·0
Uniformity coefficient D_{60}/D_{10}	1·7	1·8	2·0	2·3
Maximum void ratio e_{max}†	0·783	0·829	0·866	0·927
Minimum void ratio e_{min}†	0·523	0·470	0·487	0·465
e_{ss} at $I_1 = 10$ kPa	0·77	0·78	0·82	0·89

* Notation: 350/2 represents a median grain size D_{50} of 350 μm and a silt content of 2%.
† Determined in accordance with ASTM D2049.

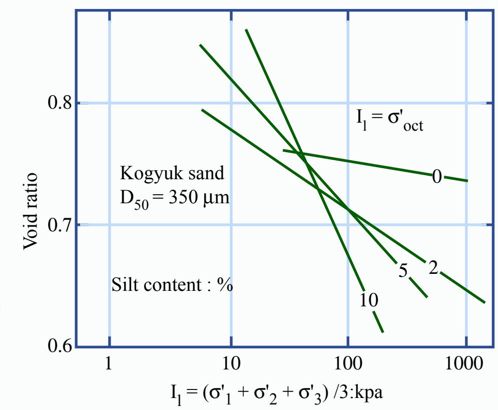

SSLs for Kogyuk 350 sand with different silt contents

Figure by MIT OCW.

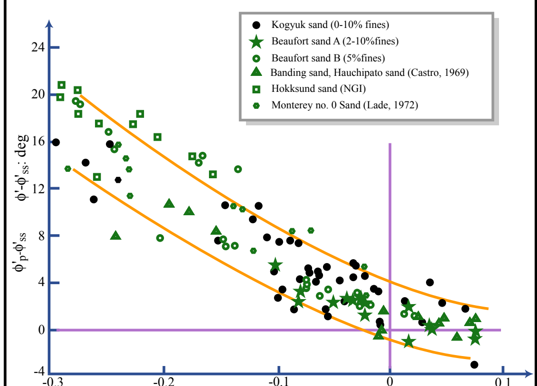

ϕ'-ϕ'$_{ss}$ as a function of state parameter

Figure by MIT OCW.

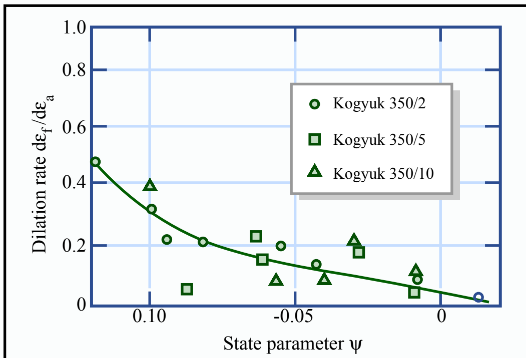

Dilation rate at peak stress ratio as a function of state parameter for Kogyuk. 350 sands.

Figure by MIT OCW.

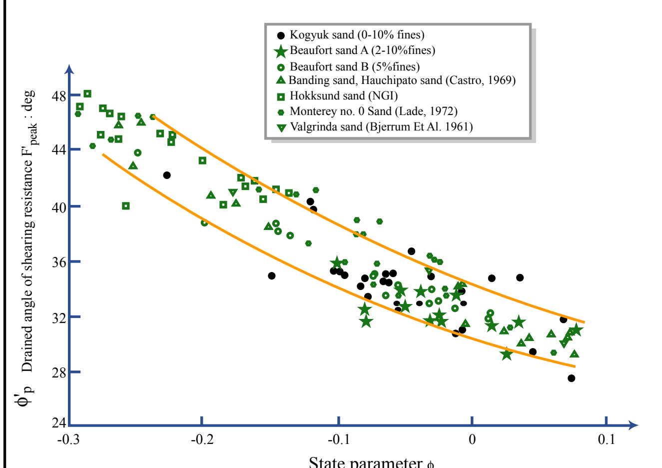

Angle of shearing resistance for several sands from the Arctic, Europe, North and South America

Figure by MIT OCW.

1st paper on State Parameter, ψ

Used Steady State Line (SSL) as reference

Data from Been, Jefferies & Hachey (1991) Géotechnique 41(3), 365-381

Table 1. Index properties of sands tested

	Erksak 330/0·7	Toyoura	Leighton Buzzard
Mineralogy			
Quartz: %	73	75	—*
Feldspar: %	22	25	
Other: %	5	0	
Median grain size D_{50}: mm	0·330	0·160	0·120
Effective grain size D_{10}: mm	0·190	0·120	0.095
Uniformity coefficient D_{60}/D_{10}	1·8	1·5	1·5
Passing 200 sieve: %	0·7	0	5
Specific gravity	2·66	2·65	2·65
Minimum density: kg/m³	1517	1338	1310
Maximum density: kg/m³	1742	1648	1592

* X-ray diffractometry was not carried out on Leighton Buzzard sand in this study. The sand consists mainly of quartz, by visual inspection.

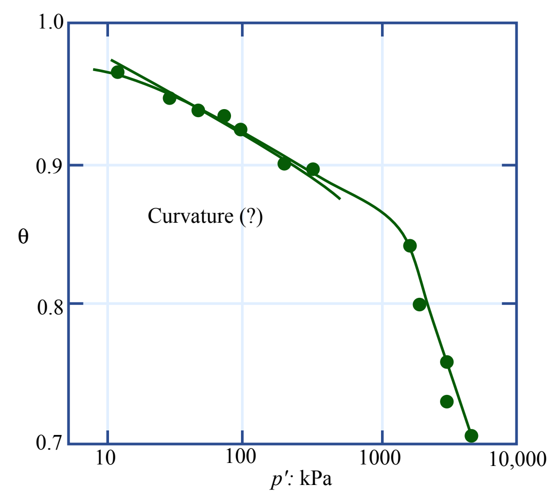

*Steady state line for **Leighton Buzzard sand** showing curvature similar to that of line for Erksak 330/0-7 sand (initial state of all samples was above the steady state line; all tests triaxial compression)*

Figure by MIT OCW.

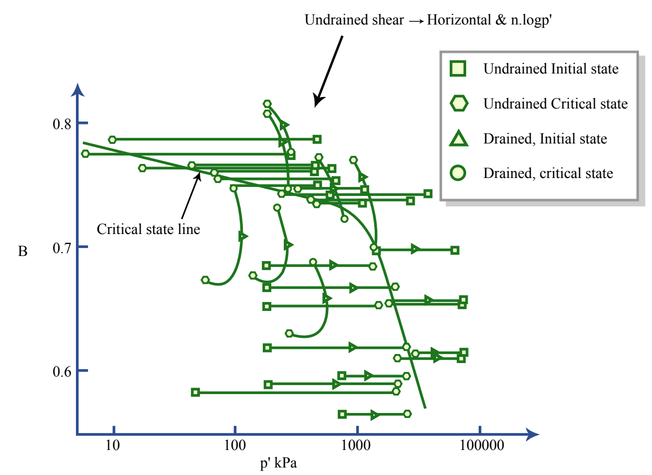

Effect of initial state on the critical state (all tests compression)

Figure by MIT OCW.

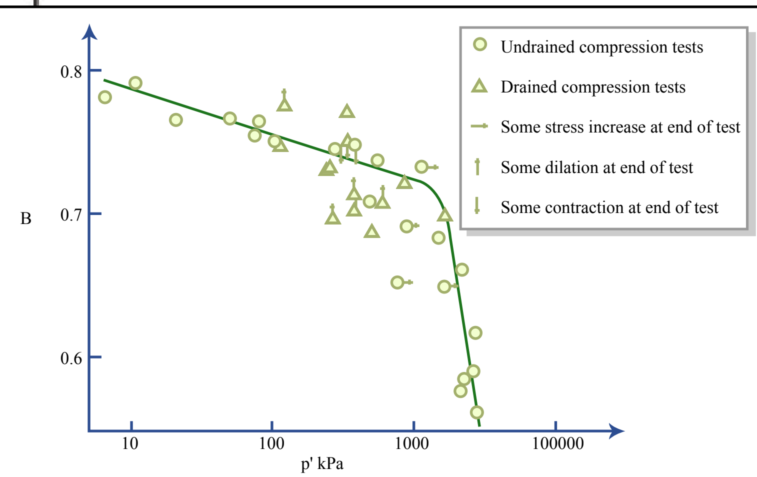

Comparison of critical state from drained and undrained tests (tests on samples consolidated to p' > 1000 kPa are not included to eliminate effect of material changes due to grain crushing during consolidation)

Figure by MIT OCW.

2nd paper on State Parameter, ψ

Concludes that Steady State Line (SSL) = Critical State Line (CSL) = shear at constant e, q & p'

Note: $p' = \sigma'_{oct}$

CCL 9/17/95 11/3/98 1.361-1.366 Part III-2

Table 1. Sand data Bolton (1986) Geot. 36(1), 65-78

Identification	Name	d_{60}: mm	d_{10}: mm	e_{min}	e_{max}	ϕ'_{crit}	Reference
A	Brasted river	0·29	0·12	0·47	0·79	32·6	Cornforth (1964, 1973)
B	Limassol marine	0·11	0·003	0·57	1·18	34·4	Cornforth (1973)
C	Mersey river	≈0·2	≈0·1	0·49	0·82	32·0	Rowe (1969)
D	Monterey no. 20	≈0·3	≈0·15	0·57	0·78	36·9	Rowe & Barden (1964) Marachi, Chan, Seed & Duncan (1969)
E	Monterey no. 0	≈0·5	≈0·3	0·57	0·86	37·0	Lade & Duncan (1973)
F	Ham river	0·25	0·16	0·59	0·92	33·0	Bishop & Green (1965)
G	Leighton Buzzard 14/25	0·85	0·65	0·49	0·79	35·0	Stroud (1971)
H	Welland river	0·14	0·10	0·62	0·94	35·0	Barden *et al.* (1969)
I	Chattahoochee river	0·47	0·21	0·61	1·10	32·5	Vesic & Clough (1968)
J	Mol	0·21	0·14	0·56	0·89	32·5	Ladanyi (1960)
K	Berlin	0·25	0·11	0·46	0·75	33·0	De Beer (1965)
L	Guinea marine	0·41	0·16	0·52	0·90	33·0	Cornforth (1973)
M	Portland river	0·36	0·23	0·63	1·10	36·1	Cornforth (1973)
N	Glacial outwash sand	0·9	0·15	0·41	0·84	37·0	Hirschfield & Poulos (1964)
P	Karlsruhe medium sand	0·38	0·20	0·54	0·82	34·0	Hettler (1981)
R	Sacramento river	0·22	0·15	0·61	1·03	33·3	Lee & Seed (1967)
S	Ottawa sand	0·76	0·65	0·49	≈0·8	30·0	Lee & Seed (1967)

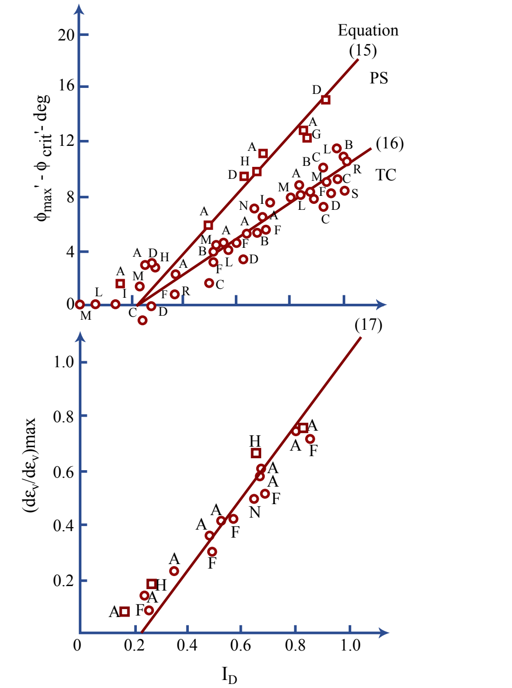

Data for sands in table 1 at failure with p' in the range 150-600 kN/m²

Figure by MIT OCW.

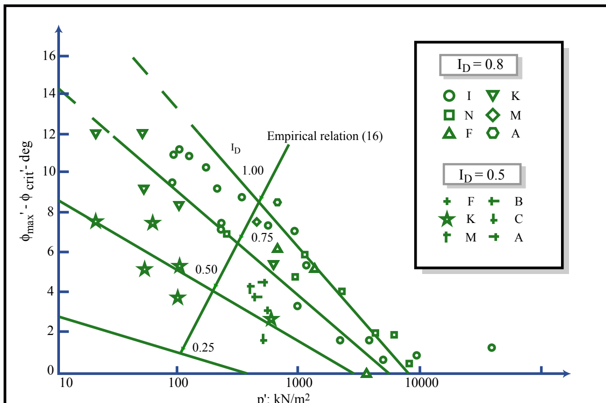

Triaxial test data for sands in table 1 failing at various mean effective stresses

Figure by MIT OCW.

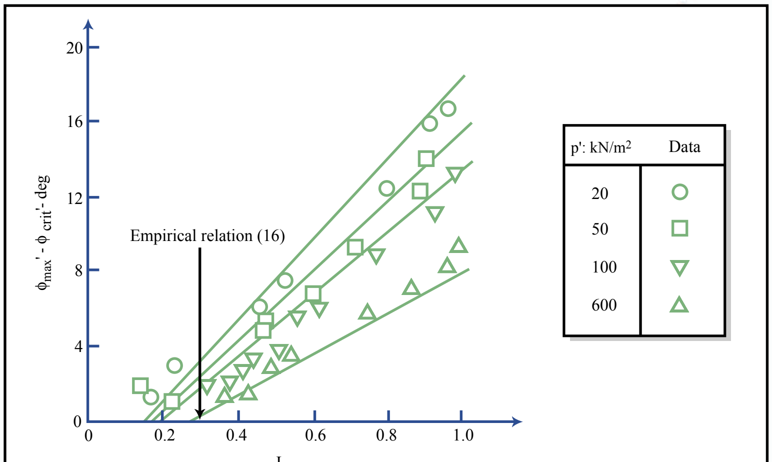

Triaxial test data for Berlin sand (K)

Figure by MIT OCW.

$\phi'_{max} = \phi'_p$; $\phi'_{crit} = \phi'_{cs}$;

$I_D \equiv D_r$; $p' \equiv \sigma'_{oct}$ at failure ;

(15) $\phi'_p(PS) - \phi'_{cs} = 5 \cdot I_R{}^{\circ}$; (16) $\phi'_p(TC) - \phi'_{cs} = 3 \cdot I_R$

(17) $(-d\varepsilon_v/d\varepsilon_a)_{max} = 0.3 \cdot I_R$ $\quad I_R = D_r\left[10 - \ln \sigma'_{oct_f}(kPa)\right] - 1$

(D)

MIT-S1 Soil Model (J. Pestana 1994 ScD Thesis)

a) Compressibility

Conventional $e - \log \sigma'_v$

Model uses $\log e$ vs. $\log \sigma'$ + LCC as reference state

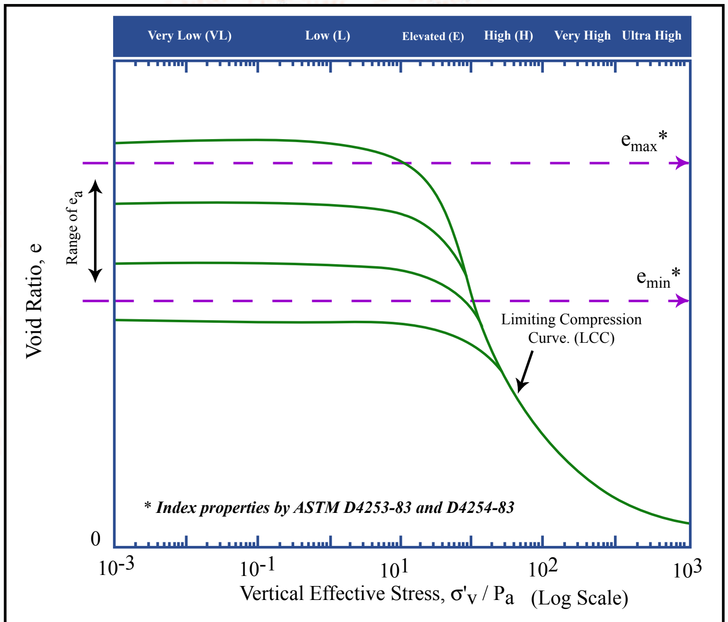

Conceptual Interpretation of Hydrostatic and One-Dimensional Compression for Freshly Deposited Cohesionless Soils.

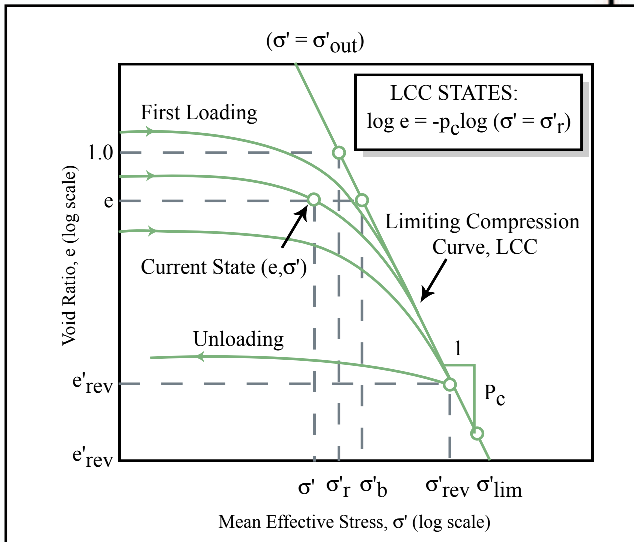

Conceptual Model Of First Loading And Unloading Of Freshly Deposited Cohesionless Soils

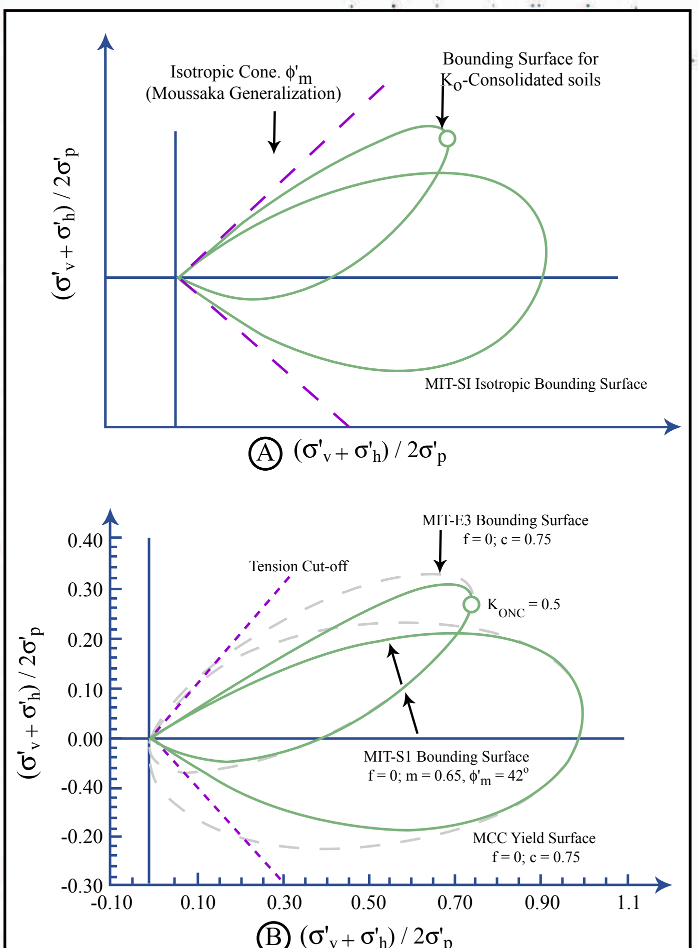

Conceptual shear behavior: a) Anisotropic and Bounding surfaces, and b) Comparison with MCC yield surface and MIT-E3 Bounding Surface.

b) Shear Behavior

Basic formulation can model both:

- Cohesive soils - uses Virgin Compression Line (VCL), i.e., σ'_p
- Granular soils - uses LCC shown Fig. 2.5

Note: MIT-E3 (Whittle 1987 ScD)

MCC → Modified Cam-Clay

Adapted from: (Roscoe & Burland 1968)

E1

Figures by MIT OCW.

Pestana (1994)

Test Type	Parameter/ Symbol	Physical contribution / meaning	Toyoura Sand
Hydrostatic or	ρ_c	Compressibility of sands at large stresses (LCC regime)	0.370
Compression Test	σ_r / p_a	Reference stress at unity void ratio for the H-LCC	55.0
(Triaxial,	θ	Describes first loading curve in the transitional regime	0.20
Oedometer)	h	Irrecoverable plastic strain, OC	-
	K_{0NC}	K_0 in the LCC regime	0.49
K_0 - oedometer	μ'	Poisson's ratio at load reversal	0.233
or K_0 -triaxial	ω	Non-linear Poisson's ratio. 1-D unloading stress path	1.00
Undrained/	ϕ'_{cs}	Critical state friction angle in triaxial compression	31.0°
Drained Triaxial Shear Tests:	ϕ'_{mr} p	Peak friction angle as a function of formation density at low stresses	28.5° 2.45
OCR=1; CIDC	m	Geometry of bounding surface. Undrained stress paths	0.55
OCR=1; CIUC	ω_s	Small strain (< 0.1%) non-linearity in shear	2.5
	ψ	Rate of evolution of anisotropy Stress-strain curves	50
Resonant Column Bender Elements	C_b	Small strain stiffness at load reversal	750

Table 5.2: MIT-S1 Input Material Parameters for Toyoura Sand.

← Input Parameters for MIT-S1 for Toyoura Sand.

- Subangular quartz, feldspar & magnetite
- $D_{50} = 0.18 \pm 0.02$ mm
- $C_u = 1.5 \pm 0.2$
- $e_{max} = 0.98$
- $e_{min} = 0.58$

} $\Delta e = 0.40$

Predicted vs. Measured Compression Behavior →

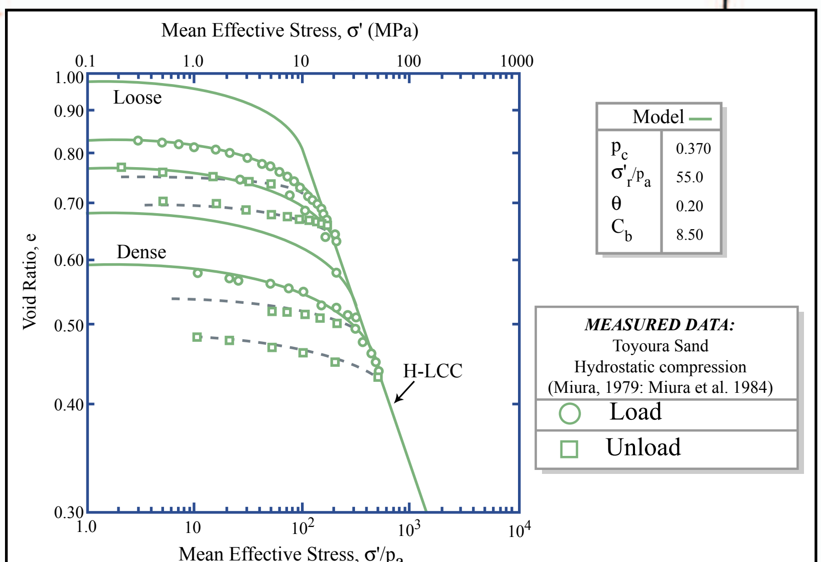

Summary of compression behavior for toyours sand

Figure by MIT OCW.

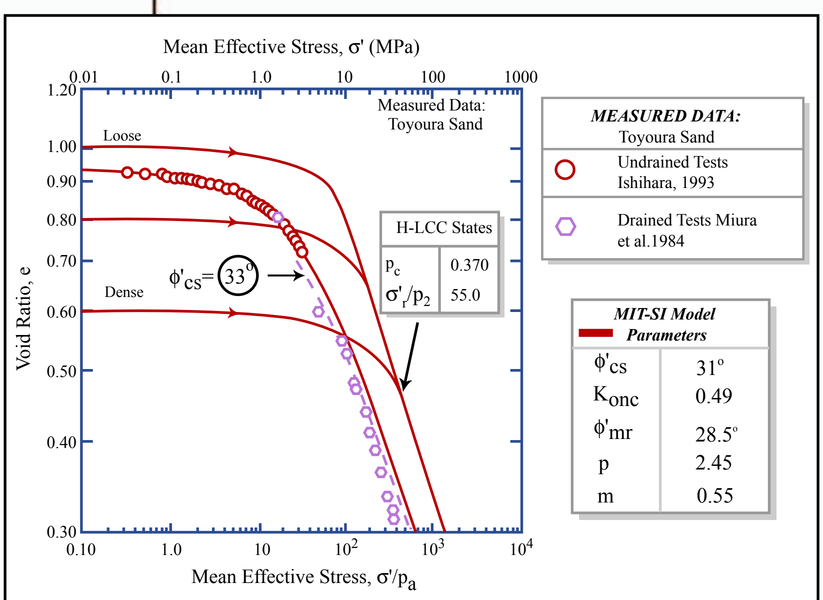

Comparison of predicted location of the critical state line with measured data for toyoura sand at high confining pressures.

Figure by MIT OCW.

← Predicted vs. Measured Location of CSL

$(\sigma' = \sigma'_{oct})$

E2

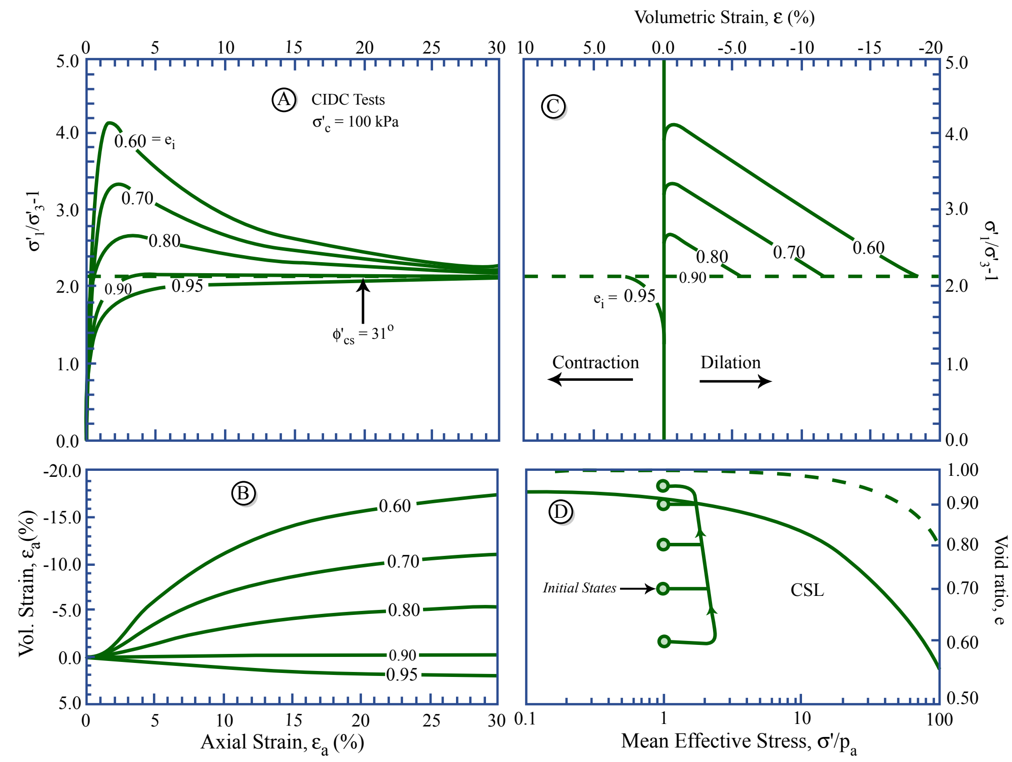

Effect of initial void ratio in the drained behavior of Toyoura sand in triaxial compression.

Figure by MIT OCW.

Effect of varying D_r at $\sigma_c' = 100$ kPa
$e_i = 0.60 \rightarrow D_r = 95\%$
$e_i = 0.90 \rightarrow D_r = 20\%$

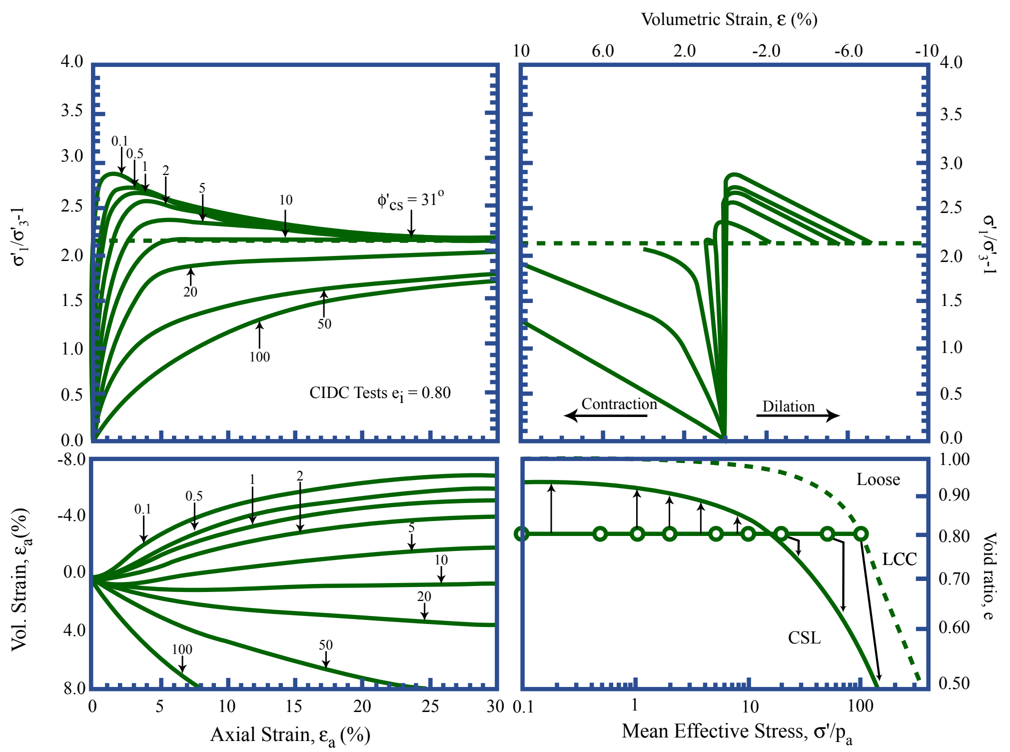

Effect of confining stress on the drained behavioyr of Toyoura sand in triaxial compression.

Initial State
Tests slopped at 40%

Figure by MIT OCW.

Effect of varying σ_c' at $e_i = 0.80$ ($D_r = 45\%$)

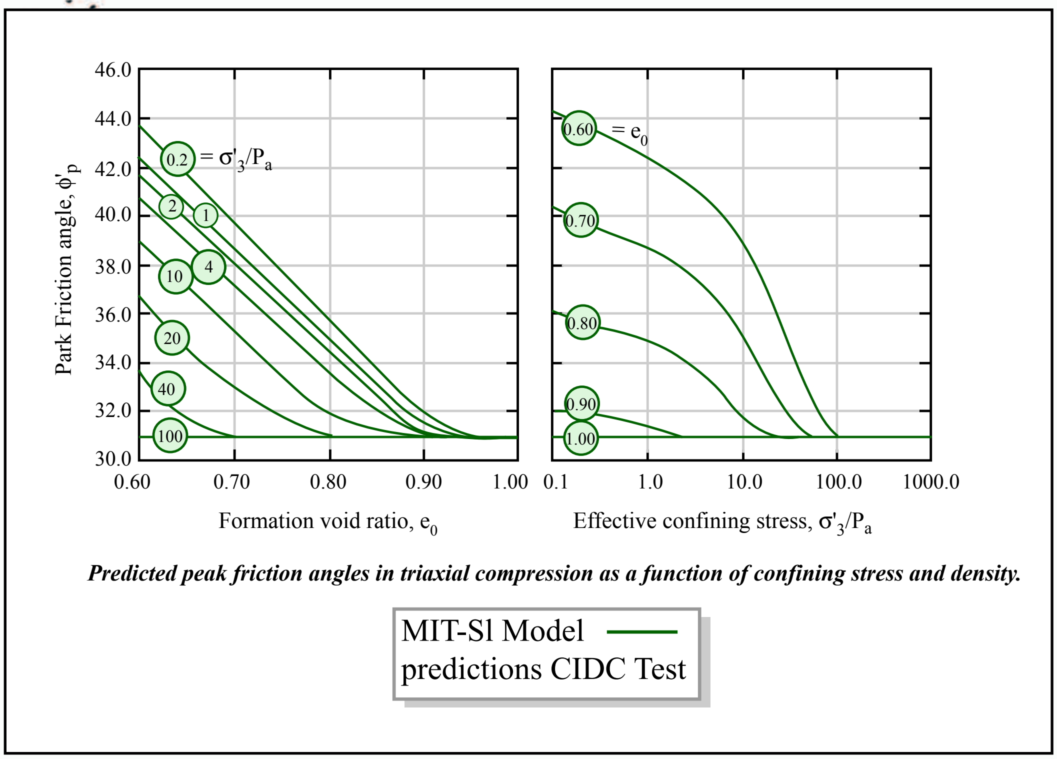

Predicted peak friction angles in triaxial compression as a function of confining stress and density.

Figure by MIT OCW.

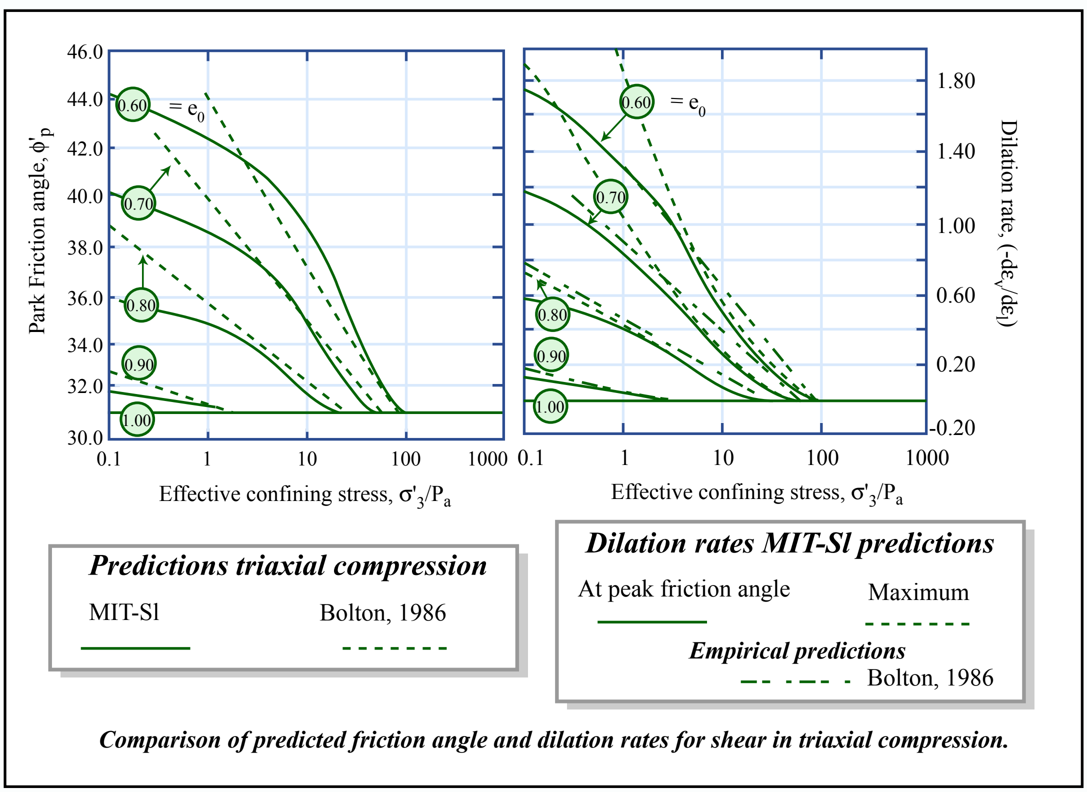

Comparison of predicted friction angle and dilation rates for shear in triaxial compression.

Figure by MIT OCW.

Toyoura Sand

Figures by MIT OCW.

Adapted from: Ladd et al. (1977) 9th ICSMFE, Tokyo

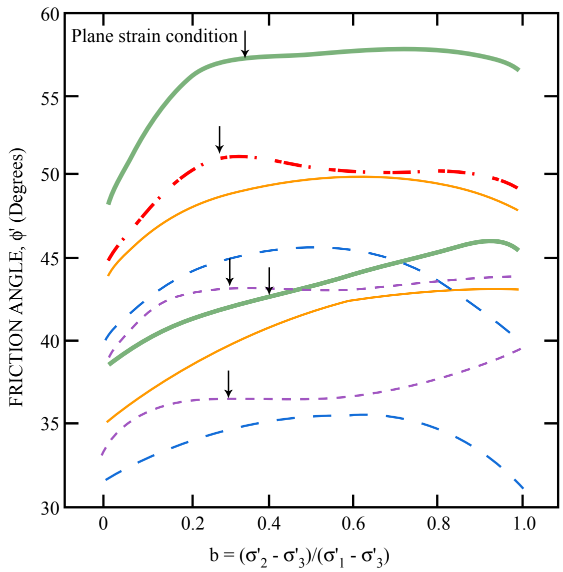

LINE	SAND	D_r(%)	REFERENCE
A_1	Ottawa	Med. loose	Ko and Scott (1968)
A_2		Med. dense	
B_1	Med Fine	30	Sutherland and Mesdary (1969)
B_2	Loch Aline	80	
C	River Welland	Dense	Proctor and Barden (1973)
D_1	Monterey Noc	27	Lade and Duncan (1973)
D_2		98	
E_2	Ham River	Loose	Reades and Green (1974)
E_1		Dense	

Effect of intermediate principal stress on the drained friction angle of several sands.

Peak ϕ vs. $b = \frac{(\sigma_2 - \sigma_3)}{(\sigma_1 - \sigma_3)}$

TC, b=0

TE, b=1

PS, b≈0.25-0.4

Figures by MIT OCW.

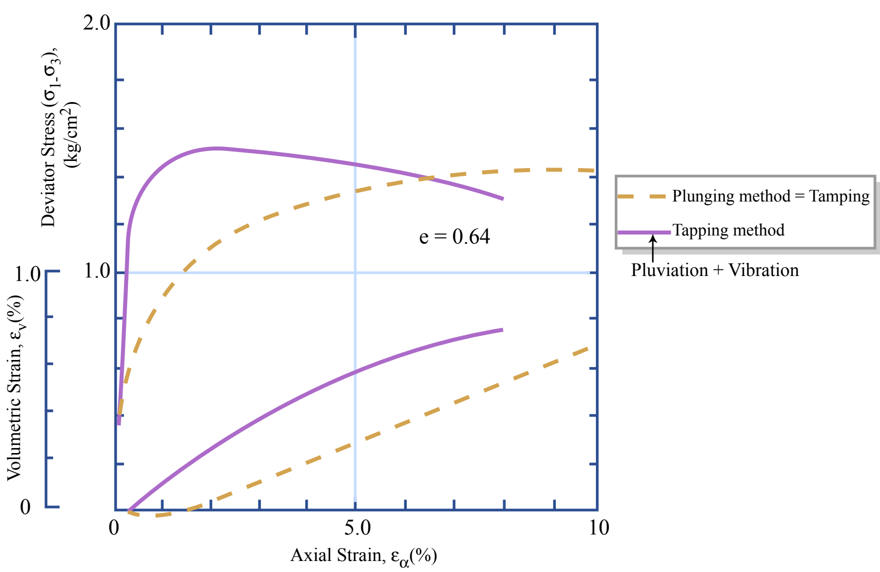

Effect of method of sample preparation on CD triaxial compression tests on Soma sand (Oda, 1972b).

Effect of Method of Sample Preparation on Drained TC Tests

F

2. UNDRAINED SHEAR : CIUC Effect of D_r & σ'_c

2.1 Toyoura Sand Data & MIT-S1 Predictions

1) Compressibility & SSL (See Fig. 5.24, Sheet E2, 1.36 Notes III-2)

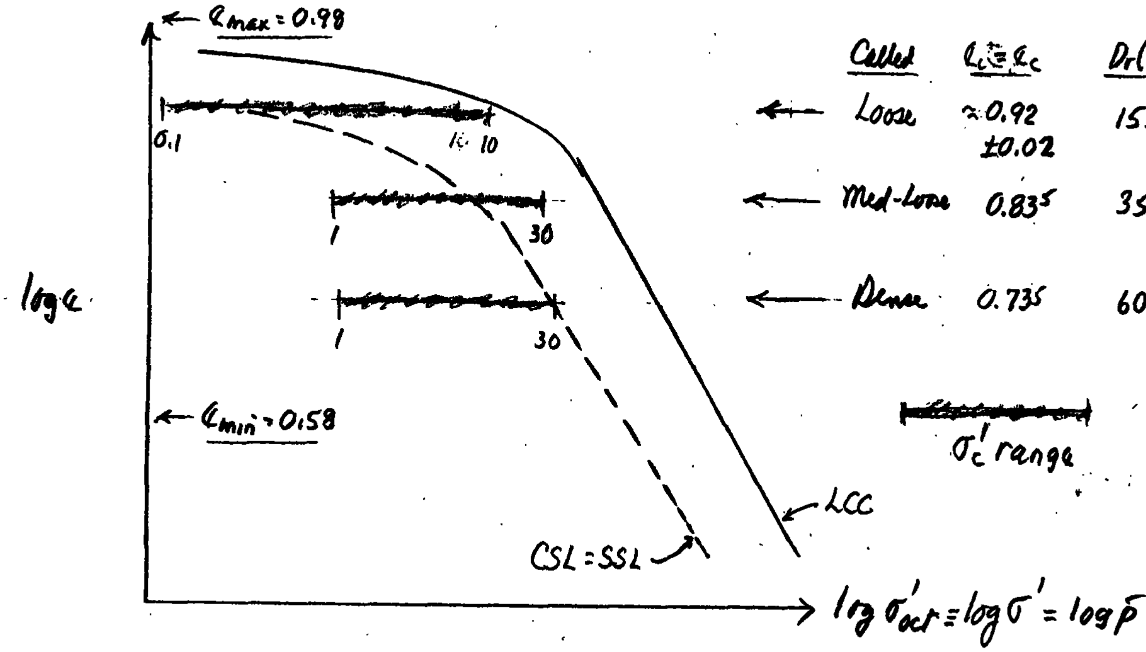

Called	$e_i \cong e_c$	D_r(%)
Loose	≈ 0.92 ± 0.02	15 ± 5
Med-Loose	0.83[5]	35
Dense	0.73[5]	60

2) "Dense" ($\psi \leq 0$) [$D_r = 60\%$]

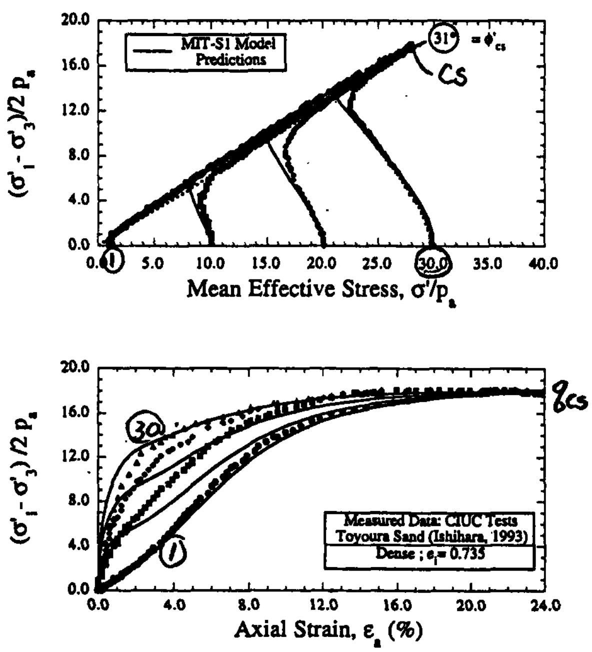

Figure 5.11: Evaluation of MIT-S1 Predictions of CIUC Tests on Dense Toyoura Sand.

- All strain hardening (SH) to q_p (peak) at CSL = q_{cs}

* Incr. σ'_c → much stiffer initial response.

- Excellent agreement (altho $\sigma'_c = 30$ test used as input)

- Same q_{cs} since same $e_i = e_c$ = constant

- "Initial yielding" when ESP changes from contractive to dilatant, i.e. when hits ESE

3) "Medium-Loose" (minus to plus ψ) [$D_r \approx 35\%$]

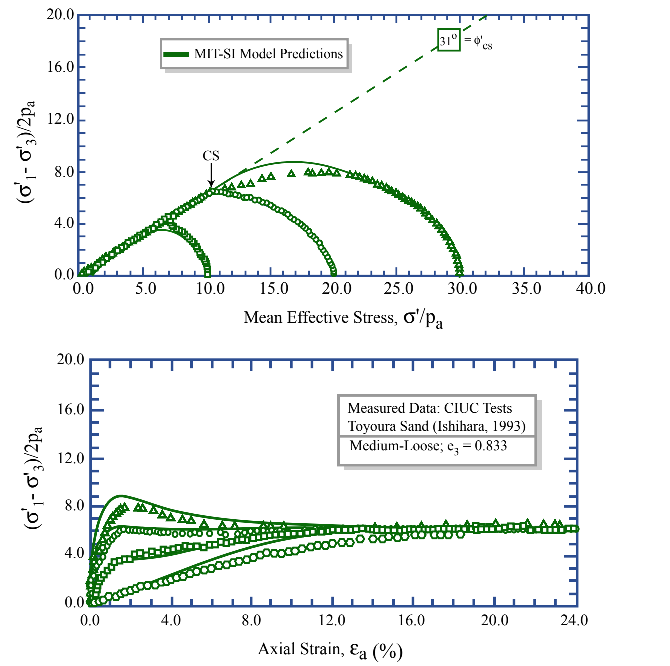

Evaluation of MIT-SI model predictions of CIUC tests on medium-loose specimens of Toyoura sand.

Figure by MIT OCW.

- $-\psi$ (low σ'_c) → SH to $q_p = q_{cs}$
- $+\psi$ (high σ'_c) → q_p at low ε_f, then SS to q_{cs}
- Excellent agreement altho. predictions → stiffer initial response
- Same q_{cs} since $e_i = e_c$ = constant

4) Loose at high σ'_c (V. high $+\psi$) [$D_r \approx 15 \pm 4\%$]

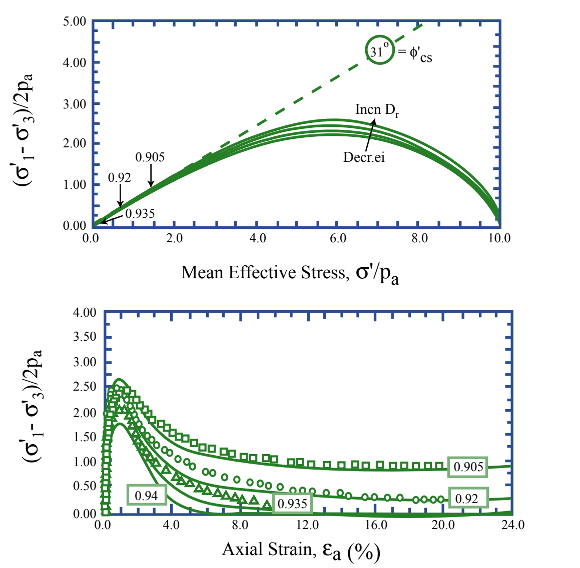

Evaluation of MIT-SI prediction of CIUC tests on loose toyoura sand at large stresses.

Measured Data: Toyoura Sand
$s'_c/p_a = 10.$

Symbol	e_1
○	0.906
□	0.933
△	0.921

Figure by MIT OCW.

- q_p at low ε_f & very low ϕ'_p

* $D_r = 15 \pm 4\% \Rightarrow \Delta D_r = \pm 4\%$

  $q_p/\sigma'_c = 0.25 \pm 0.02$ small range

  $q_{cs}/\sigma'_c = 0.05 \pm 0.05$ LARGE range

- Excellent predictions

* $D_r \approx 10\%$ ($e_i \approx 0.94$) → LIQUEFACTION ($q_{cs} \approx 0$)

- Failure → FLOW SLIDES when have small q_{cs}

5) Quasi-Steady State (QSS): Loose with varying σ_c'

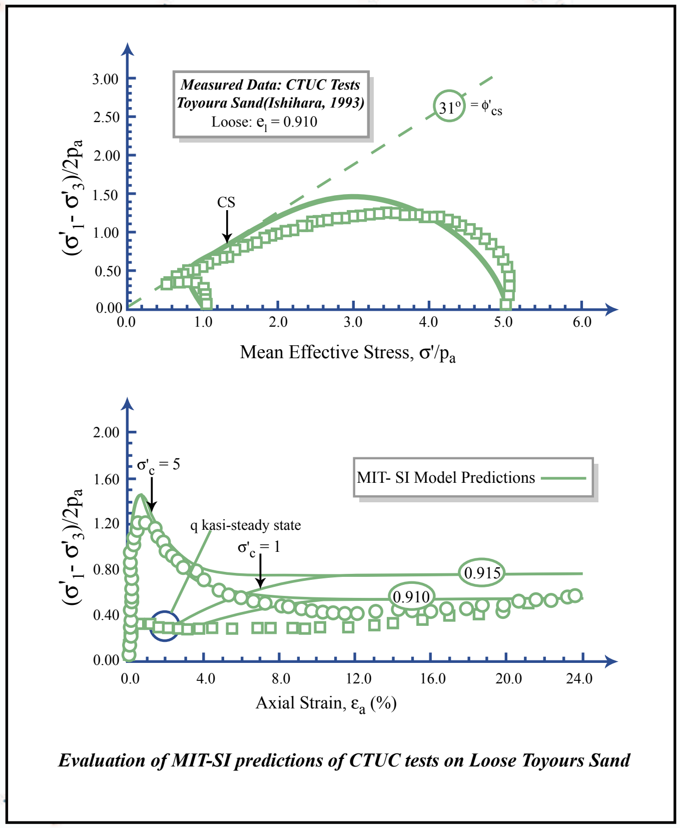

Figure by MIT OCW.

- High σ_c' → dilat SS after q_p ($\sigma_c'=5$)
- Low σ_c' → ($\sigma_c'=1$)
  - Initial "peak" = q_Y (yielding)
  - SS to give min q at quasi-steady state (QSS)
  - q_{min} occurs when ESP changes from contractive to dilatant
  - then SH → q_{cs}

Will use p4 for details

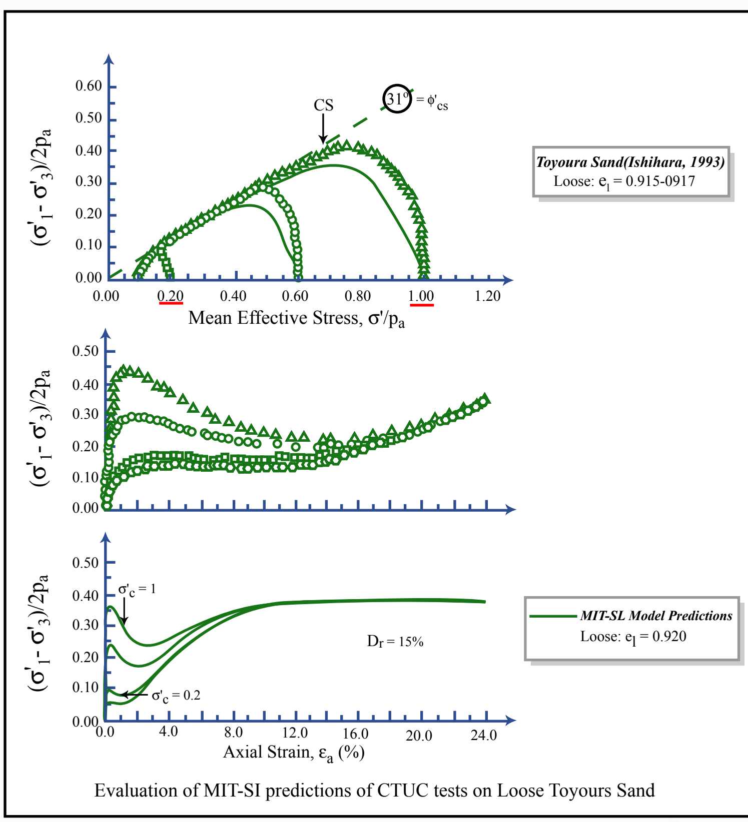

Figure by MIT OCW.

- Shows effect of varying σ_c' at low stresses (0.1-1 bar)
- Increasing σ_c' →
  - large increase in 1st peak = q_Y
  - larger SS to reach q_{min}
  - then SH to q_{cs}
- Predictions show more rapid SS to SH behavior than measured (but still amazing agreement)

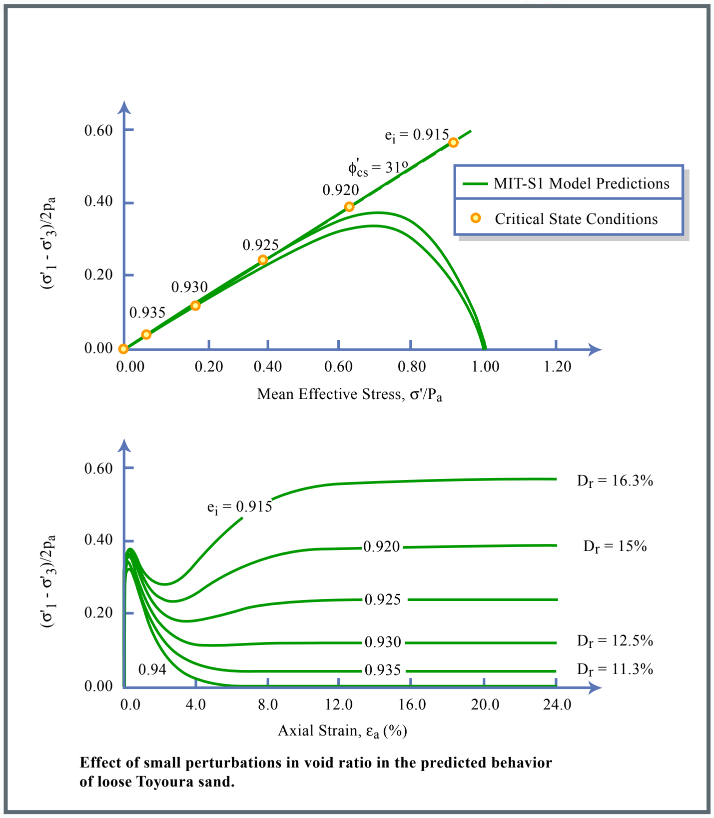

Effect of small perturbations in void ratio in the predicted behavior of loose Toyoura sand.

Figure by MIT OCW.

- Further illustration of sensitivity of post q_{yield} behavior due to small Δe ($\Delta D_r \approx 5\%$).
- 1st peak: $q_y/\sigma'_c = 0.37 \pm 0.01$
- Large strain: $q_{cs}/\sigma'_c = 0.04 - 0.57$

Large range very important for liquefaction & flow slides

6) Ishihara [1993 - Geot, 33rd Rankine Lecture 43(3)]

Toyoura Sand

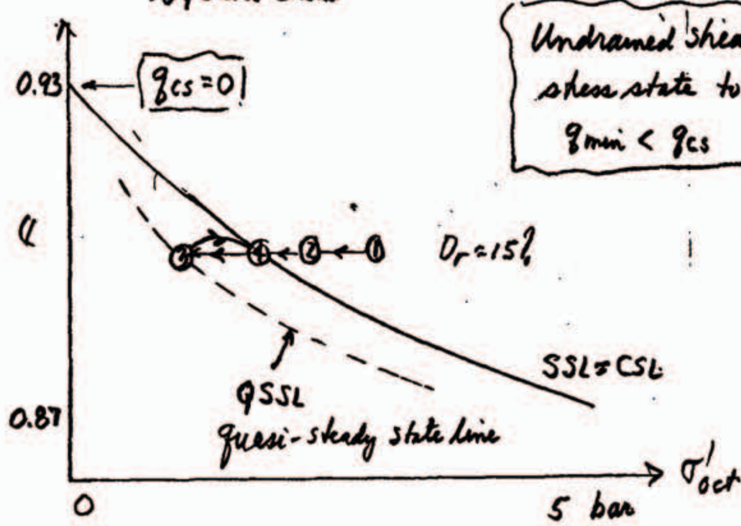

Undrained shear from +ψ can lead to stress state to left of CSL with $q_{min} < q_{cs}$

③ = "phase change": from contractive to dilatant behavior

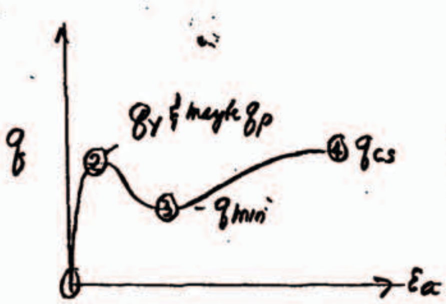

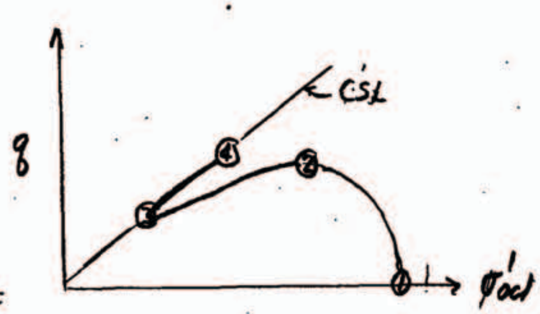

2.2 MIT Data on MFS (Swan 1994 ScD)

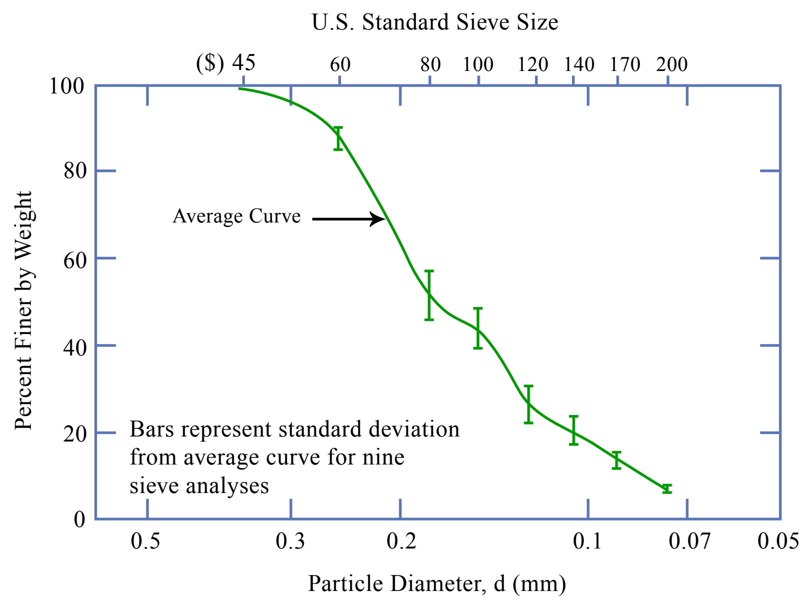

MFS Parameters

d_{50} = 0.18 mm
C_c = 1.08
G_s = 2.688 ± 0.003
γ_{dmax} = 1.701 g/cm^3
(ASTM D4254 Method A)
γ_{dmin} = 1.408 g/cm^3
(ASTM Method 1.A)

Grain Size Distribution of Manchester Fine Sand

Figure by MIT OCW.

- MFS-4,5 Stress-strain & ESP : Effect of incr. σ_c' for dense sand (Trends agree w/ Fig 5.11 Toyoura sand) p1
- MFS-6,7 " " " : Effect of incr. D_r at σ_c' = 20 bar (Test C-15 almost shows @ SS condition)
- MFS-8 Definition of SSL from CIUC tests
- MFS-9 A_f vs ψ for CIUC tests → very consistent trend
- MFS-10 Log q_f/σ_c' vs ψ for CIUC tests → linear relationship

3. UNDRAINED SHEAR: OTHER FACTORS

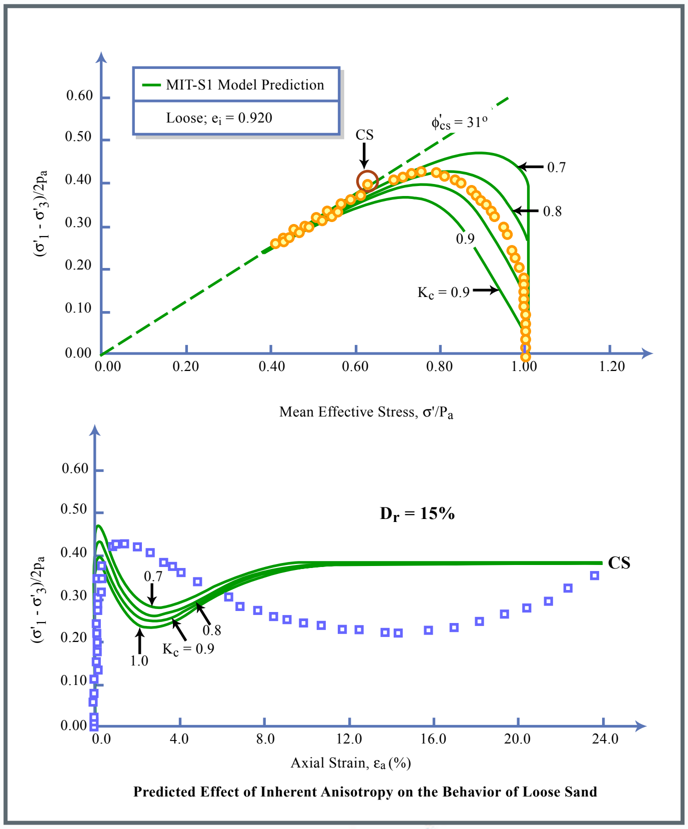

Figure by MIT OCW.

3.1 Inherent Anisotropy

1) Effect of anisotropic consolidation
   - Specimens consolidated along $K_c = 1.0$ to 0.7 ESP →
   - inherent anisotropy
   - Specimen unloaded at const. σ'_{oct} to $K=1$
   - Then CIUC shear

2) Results for v. loose at $\sigma'_c = 1$ bar
   - Large ΔESP
   - Smaller change in q vs ε_a ($q_p/\sigma'_c = 0.35 \rightarrow 0.45$)
   - again MIT-S1 → more rapid SS to SH behavior than measured
   - Same q_{cs} since constant $e_i = e_c$

Inherent anisotropy → less contraction and higher q_f/σ'_c

3.2 CIU vs CAU: TC & TE

- See p7 (Fig 5.23) MIT-S1 predictions for Toyoura Sand :: $e_i = 0.80$

Large + ψ { $D_r = 45$% ; $(\sigma'_{oct})_c = 50$ bar }

Test	q_f	σ'_{vc}	q_f/σ'_{vc}	
CIUC	15	50	0.30	} Similar to clays
CAUC	22.5	75	0.30	
CIUE	12	50	0.24	← −20% vs. CIUC } Similar to clays
CAUE	11	75	0.15	← $K_s = 0.15/0.30 = 0.5$ } like lean clay

MIT-S1 predictions for Toyoura Sand ($D_r = 45\%$)

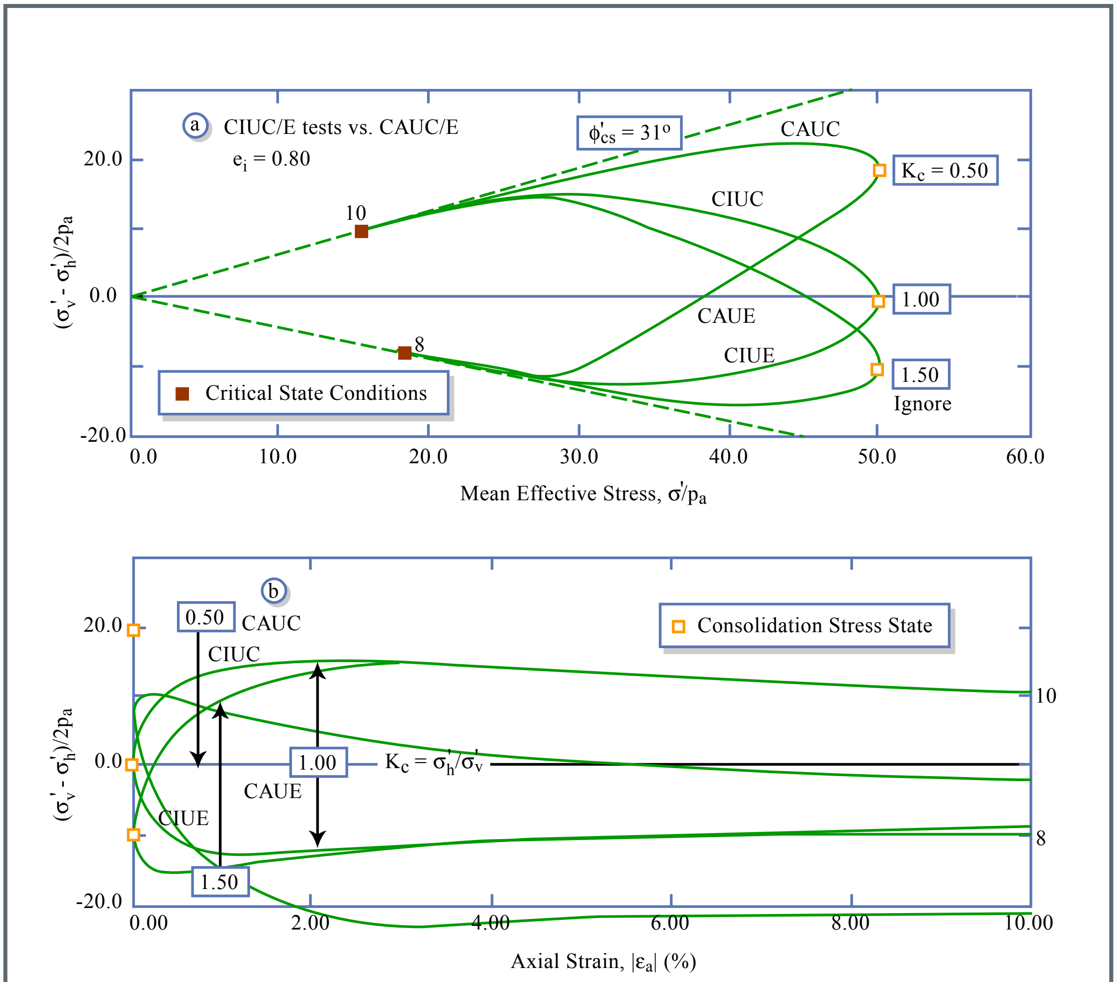

Effect of Consolidation Stress History on the Triaxial Compression/Extension Behavior

Figure by MIT OCW.

Questions: 1) Why do CIUC & CAUC → same q_{cs}?

2) Why do CIUE & CAUE → lower q_{cs}?

3) Compute MIT q/p' at peak & CS

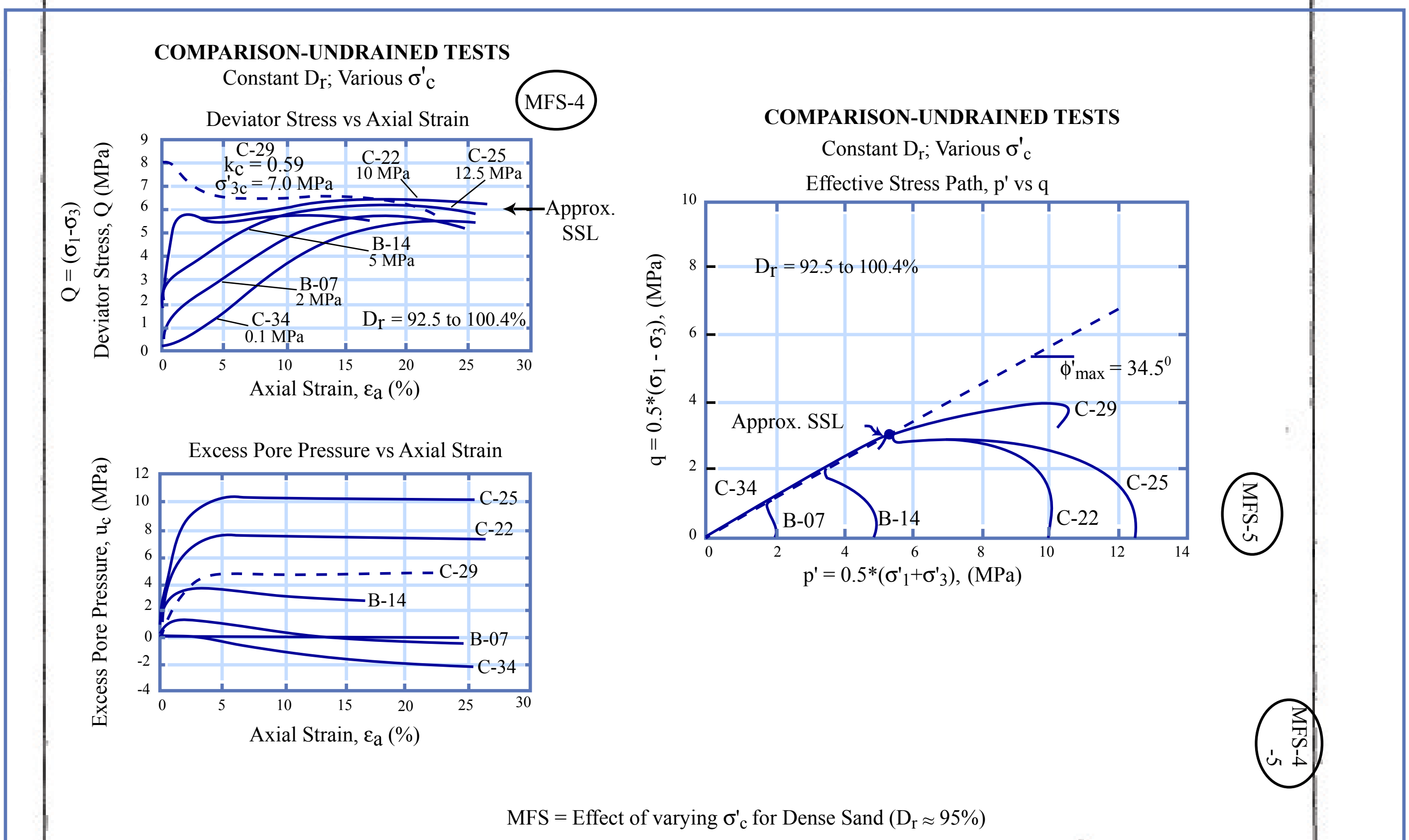

Figure by MIT OCW.

MFS-6/-7

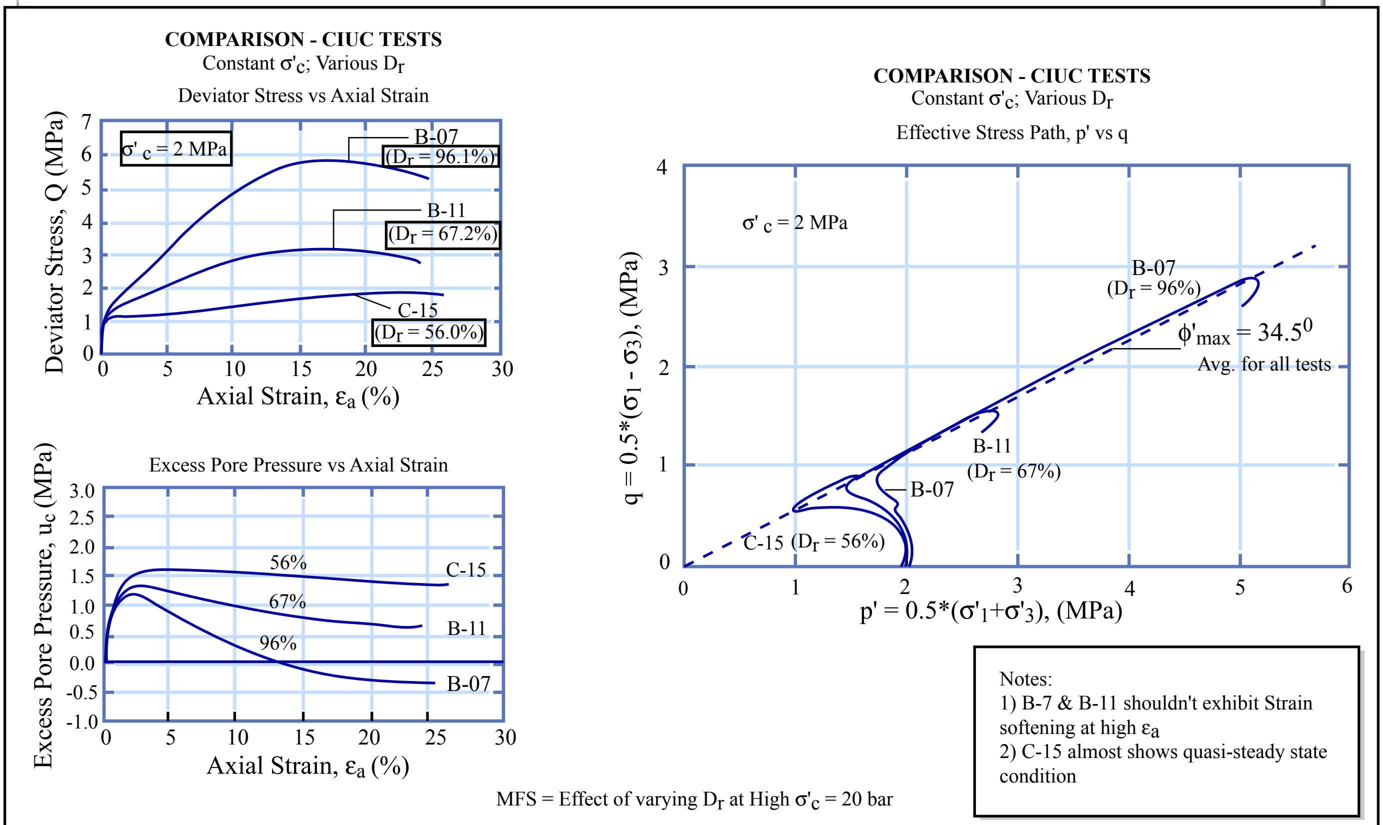

Figure by MIT OCW.

25

CCL 4/21/96
1.322

MFS-8

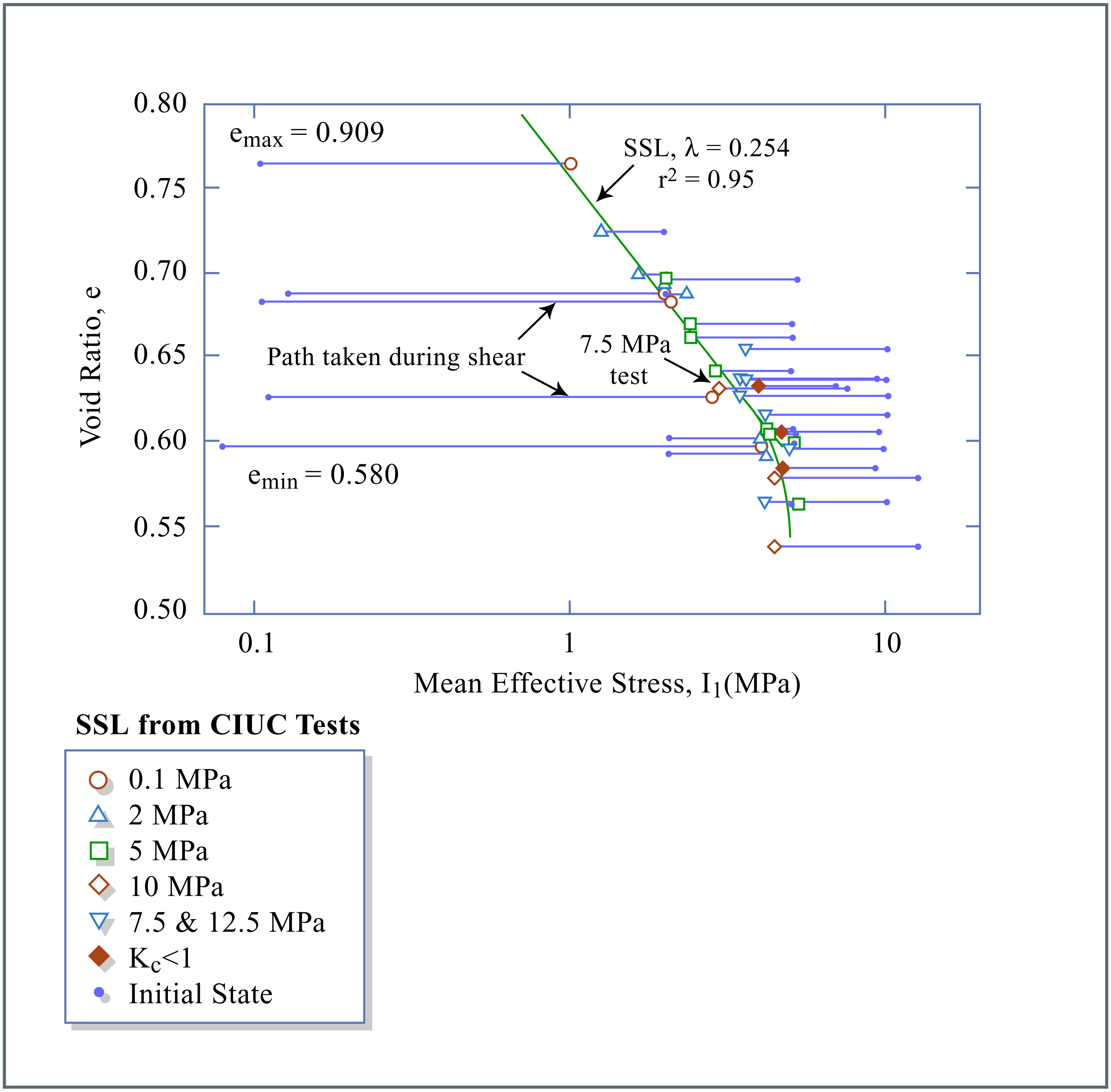

Figure by MIT OCW.

3/31/94
CWS

CCL 4/26/94
1.322

MFS-9

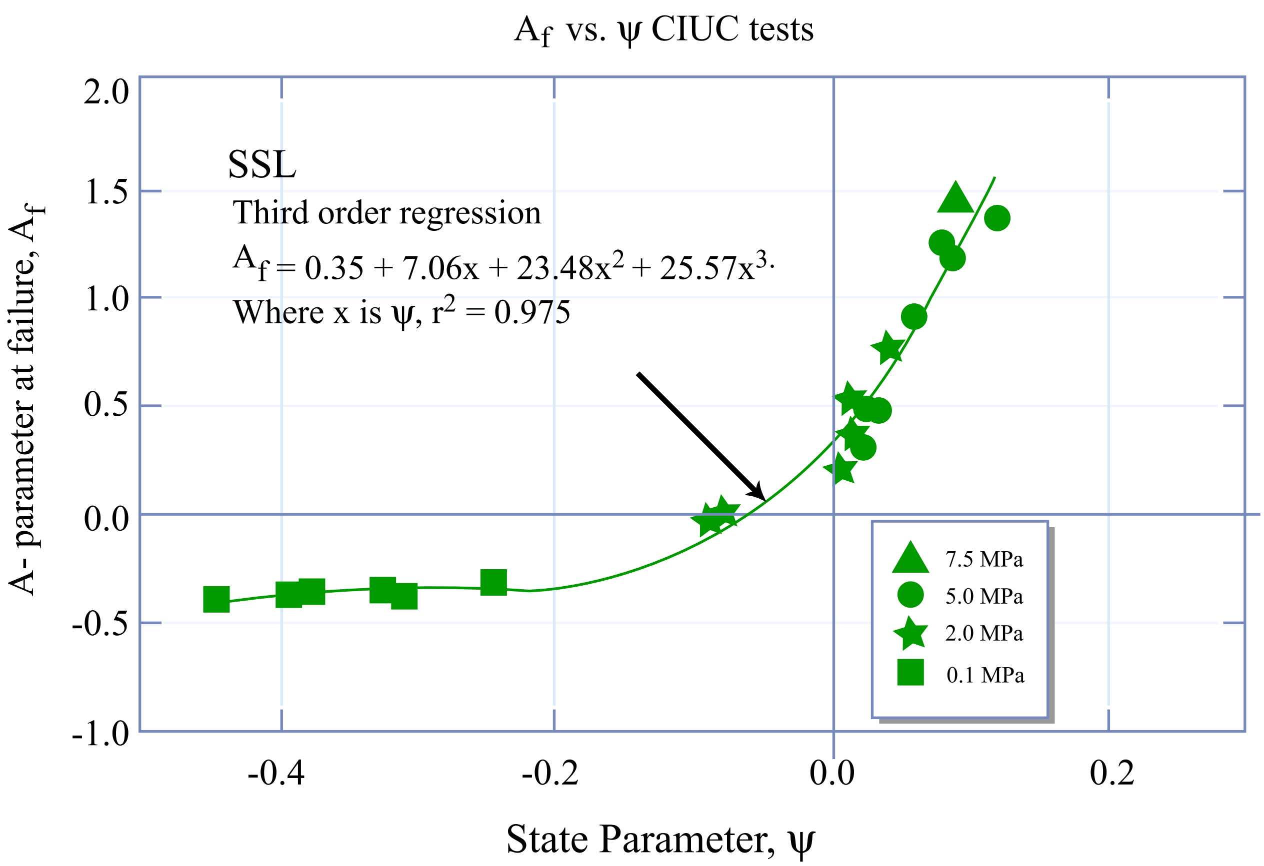

Figure by MIT OCW.

AFSSL.SP5

2B

3/31/94
CWS

CCL 4/26/94
1.322

MFS-10

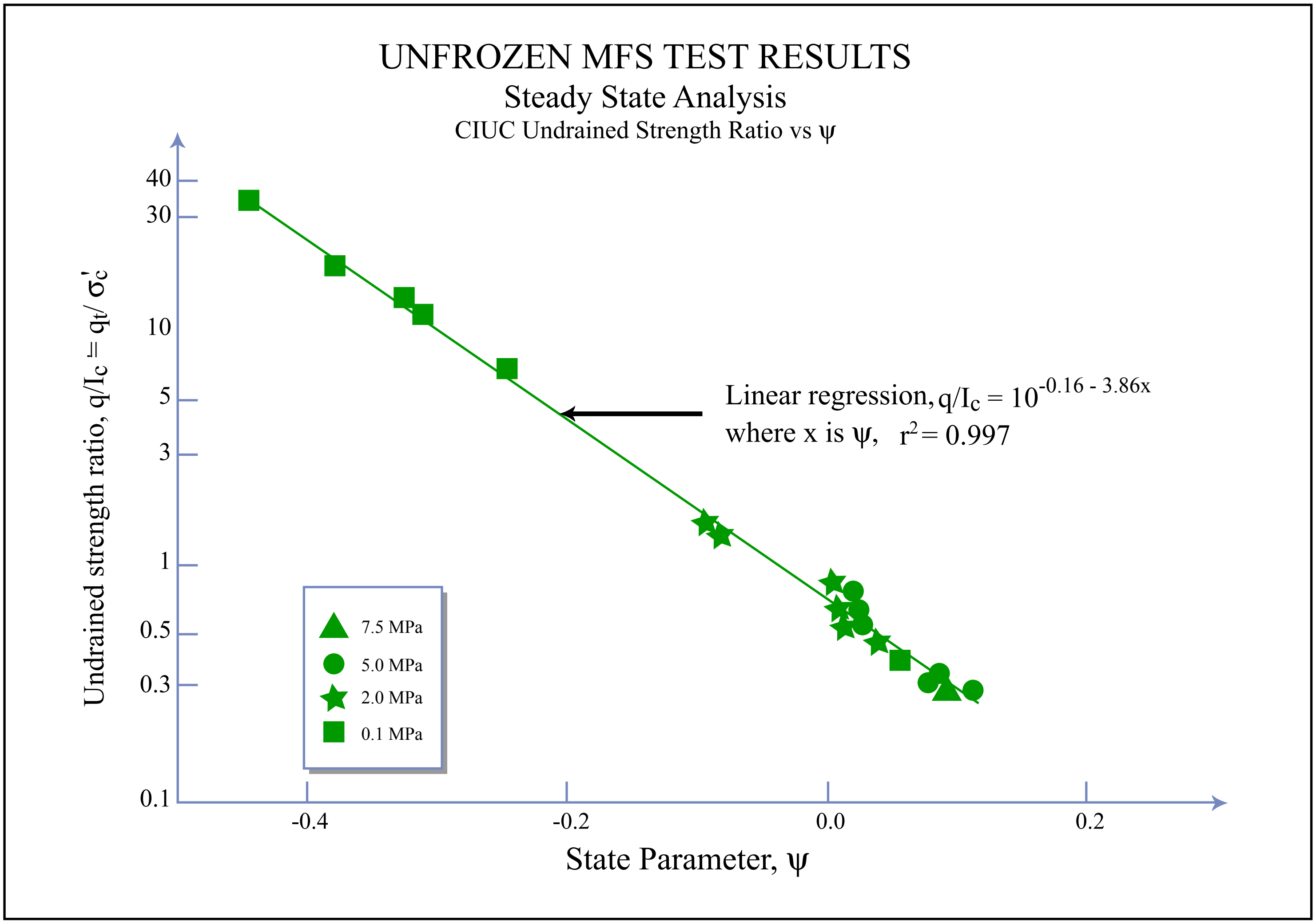

Figure by MIT OCW.

USRSSL.SP5